Aalto University
School of Chemical
Technology

Tommi Juhani Rinne

THE UTILIZATION OF HYDROXYPROPYL METHYLCELLULOSE AS A FLOTATION FROTHER FOR CHALCOPYRITE-CONTAINING ORES

Master's Programme in Chemical, Biochemical and Materials Engineering
Major in Functional Materials

Master's Thesis for the degree of Master of Science in Technology
Submitted for inspection, Espoo, 11th October, 2018

Supervisor	Assistant professor Rodrigo Serna-Guerrero
Advisor	Master of Science (Technology) Ted Nuorivaara

Aalto University
School of Chemical Engineering

Author Tommi Juhani Rinne	

Title of Thesis The Utilization of Hydroxypropyl Methylcellulose as a Flotation Frother for Chalcopyrite-Containing Ores

Degree Programme Chemical, Biochemical and Materials Engineering

Major Functional Materials   **Code of Major** CHEM3025

Thesis Supervisor Assistant Prof. Rodrigo Serna-Guerrero

Thesis Advisor M.Sc. (Tech.) Ted Nuorivaara

Date 11.10.2018   **Number of Pages** 104+ 15 **Language** English

Abstract

Froth flotation is a widely applied mineral separation technique, in which minerals are enriched in a complex three-phase system (froth) that comprises of air-, liquid-, and solid phases. In the flotation process, a variety of reagents are needed to control the chemical environment of the process, and to provide the basis for the separation to happen. Frothers, which are flotation chemicals used to control the properties of air bubbles, are an example of such reagents. Recently, efforts have been made to improve the environmental performance of flotation by replacing some of the industrially applied hazardous reagents by more sustainable alternatives.

In this master's thesis, a sustainable cellulose-based frother (hydroxypropyl methylcellulose, HPMC) was studied and compared to a commercially available frother. The aim of this thesis was to understand the theory of flotation, the theory of macromolecular frothers, and the role of frothers in the flotation process in general. Furthermore, in the experimental section, an effort was made to optimize the flotation parameters for chalcopyrite separation from a pyrite-rich Cu-Zn ore, utilizing HPMC as a frother. A total of 53 experiments were conducted, studying two distinctive types of HPMC both singularly, and in mixtures with the commercial frother. Furthermore, reference experiments were conducted utilizing the commercial frother only.

HPMC was found to produce very stable froths at concentrations exceeding 30ppm, and the kinetics of the HPMC-based separation were observed to be superior compared to the commercial frother. Furthermore, on its own HPMC produced very high recoveries of the valuables but failed to separate them selectively. However, when applied in mixtures with the commercial frother, the selectivity of the process could be improved, while the high recovery values were maintained (also with HPMC concentration well-below the 30ppm threshold point). In the experiments, the best separation efficiency obtained with a mixture was 69.51%, whereas the commercial frother performed slightly better at 74.67%. These values were not yet on an industrially acceptable level (due to poor pyrite depression) but they were still comparable with one another. Although further research is needed, based on these results it can be stated that HPMC seems to be a potential alternative, when it comes to improving the environmental performance of flotation.

Keywords froth flotation, frothers, chalcopyrite, hydroxylpropyl methylcellulose, hypromellose, HPMC

Tekijä	Tommi Juhani Rinne
Työn nimi	Hydroksyylipropyyli-metyyliselluloosa vaahdotteena kuparikiisun vaahdotuksessa
Koulutusohjelma	Kemia, bioteknologia ja materiaalitekniikka
Pääaine	Toiminnalliset materiaalit **Pääaineen koodi** CHEM3025
Työn valvoja	Apul. Prof. Rodrigo Serna-Guerrero
Työn ohjaaja	DI Ted Nuorivaara
Päivämäärä 11.10.2018	**Sivumäärä** 104 + 15 **Kieli** englanti

Tiivistelmä

Vaahdotus on mineraaliteollisuuden yleisesti hyödyntämä erotusmenetelmä, jossa haluttu mineraali rikastetaan vaahdoksi kutsuttuun ilman, veden ja kiinteän aineen muodostamaan kolmifaasisysteemiin. Vaahdotuksessa tarvitaan useita kemikaaleja, joilla kontrolloidaan prosessin olosuhteita ja luodaan pohja halutun mineraalin rikastumiselle. Esimerkki tällaisista kemikaaleista ovat vaahdotteet, joilla säädellään vaahdon ilmakuplien ominaisuuksia. Viime aikoina vaahdotuksen ympäristösuorituskykyä on pyritty parantamaan tutkimalla ympäristölle edullisia vaihtoehtoisia vaahdotuskemikaaleja nykyisten osittain toksisten kemikaalien korvaajina.

Tässä diplomityössä tutkittiin ekologista selluloosapohjaista vaahdotinkemikaalia (HPMC), sekä vertailtiin sen suorituskykyä kaupalliseen vaahdottimeen. Työn tavoitteena oli ymmärtää vaahdotuksen ja suurimolekyylisten vaahdotteiden teoriaa, sekä vaahdotteiden yleistä merkitystä vaahdotusprosessissa. Lisäksi kokeellisessa osuudessa pyrittiin optimoimaan vaahdotusparametrit kuparikiisun erottamiseksi pyriittipitoisesta kupari–sinkki-malmista, käyttäen HPMC-vaahdotetta. Työssä suoritettiin 53 vaahdotuskoetta, joissa tutkittiin kahta erilaista HPMC-vaahdotetta niin yksittäin, kuin sekoitettuna kaupalliseen vaahdottimeen. Lisäksi kaupallisella vaahdottimella suoritettiin referenssikokeita.

HPMC:n todettiin muodostavan hyvin stabiileja vaahtoja tietyn kynnyksen ylittävissä konsentraatioissa (30ppm), sekä sen erotuskinetiikan huomattiin olevan huomattavasti kaupallista vaahdotetta nopeampi. Pelkällä HPMC:llä kyettiin myös huomattavan suuriin kuparikiisun talteenottoihin, mutta selektiivisyys ei ollut toivotulla tasolla. Sen sijaan sekoittamalla HPMC:tä ja kaupallista vaahdotinta saatiin selektiivisyyttä parannettua, talteenoton pysyessä korkealla (myös hyvin pienillä HPMC-konsentraatioilla). Suoritetuissa kokeissa sekoituksilla saavutettu paras erotustehokkuus oli 69,51%, kun se kaupallisella vaahdottimella oli hieman parempi 74,67%. Arvot eivät vielä olleet teollisesti hyväksyttävällä tasolla (johtuen pyriitin painamisen hankaluudesta), mutta ne olivat silti keskenään vertailukelpoisia. Vaikkakin lisätutkimuksia vielä tarvitaan, voidaan jo nyt todeta, että HPMC on varteenotettava vaahdotinkemikaali vaahdotuksen ympäristösuorituskyvyn parantamiseen tähtäävässä tutkimuksessa.

Avainsanat vaahdotus, vaahdotteet, kuparikiisu, hydroksipropyyli-metyyliselluloosa, hypromelloosi, HPMC

Table of Contents

1   Introduction

Since its commercial introduction in the early 20th century, froth flotation has become the most important and widely used separation technique in the mineral industry [1]. During the past 100 years, its development has enabled the utilization of complex and low-grade ores and thus, allowed the industry to answer the ever-growing demand for mineral-based raw materials [2]. At the same time, it has become increasingly evident that the environmental impacts of mineral processing cannot be neglected. There is a strong consensus that the processes and technologies of the future must satisfy a greener and cleaner standard, in addition to providing a basis for economic growth [3].

Froth flotation is a chemically intensive process, in which a variety of reagents are utilized to provide the optimal conditions for the separation of the valuable minerals. These reagent chemicals are essential for flotation, and the failure to apply them properly results in an inefficient performance, and an unprofitable process. [4] Many of these chemicals, however, can be toxic and environmentally hazardous. This is true for example regarding xanthates (used as collectors) [5], but also with many other commercial flotation reagents, including frothers. One strategy of improving the environmental performance of flotation, is to study green alternatives for the currently used chemicals.

Cellulose is a common organic polymer found everywhere in nature. It is the main skeletal component of all advanced plant life, and an estimated 1.5×10^{12} metric tons of it is produced annually by natural organisms. Due to these huge volumes, cellulose

is considered a virtually inexhaustible raw material for green and biocompatible products. [6]

An interesting aspect of cellulose is that its properties can be tailored by controlling the chemical nature of the repeating monomer units [7]. These types of modified cellulose structures are known as cellulose derivatives, and they have found usage regarding many applications, including membranes, films, coatings, pharmaceuticals, and foodstuffs [6]. Also, the foam stabilizing ability of cellulose ethers has long been known [8]. Recently, a cellulose derivative known as hydroxypropyl methylcellulose (HPMC) has been demonstrated to show some promising behavior as a flotation frother, and pioneering experimentation for its usage in the flotation process has been done [9].

In this master's thesis, a cellulose-based HPMC frother was studied and compared to a commercial frother chemical. The aim of this thesis was to understand the theory of flotation, the role of frothers in a flotation system, and the working principle of a macromolecular frother – in this case HPMC. Also, this thesis targeted to review cellulose derivatives in a more general sense, and their structures, properties, and applications on other fields were studied as well. Regarding this literature review, HPMC was again given the most notice. Furthermore, in the experimental part, an effort was made to optimize the flotation parameters for chalcopyrite ($CuFeS_2$) separation from a pyrite-rich Cu-Zn ore, utilizing HPMC as a frother.

In the theoretical section, chapter 2 offers a brief review on the well-established flotation fundamentals. Chapter 3 then provides review of cellulose and cellulose derivatives – focusing especially on HPMC. In this chapter, the main focus is kept on the theory and utilization of HPMC in the context of flotation, although the general properties, synthesis, and applications of other cellulose derivatives are discussed as well. The experimental section then shifts on to study the HPMC frother in a laboratory scale flotation setup. In chapter 4, the materials and methods are first introduced, along with an experimental plan, and a walkthrough of the process of an individual experiment. Results are given in chapter 5, and subsequently discussed in chapter 6. Finally, chapter 7 summarizes the thesis, and makes suggestions for further research.

2 Froth Flotation

This chapter introduces the reader to the fundamental concepts of froth flotation. First, a quick overview of the general flotation principles is made. Then an explanation for the physical basis of the separation by flotation (hydrophobicity) is given, along with explaining the performance limiting factors of the process (grade-recovery). Lastly, the chapter discusses flotation reagents, of which frothers are presented in most detail.

2.1 General Principle of Flotation

Flotation is a widely used mineral separation technique in which the differences in the physico-chemical surface properties of different minerals are utilized to achieve a selective separation of the valuables from the gangue. During the flotation process, minerals are enriched in a complex three-phase system known as froth, which

comprises of a solid phase (mineral particles), a liquid phase (water), and a gas phase (air). The flotation process takes place in a flotation cell as air is blown into a solid-water suspension (pulp) and, due to strong agitation, air bubbles start colliding with mineral particles, which then attach onto the bubble surfaces. The mineralized bubbles then rise to the top, forming the froth, which can be scooped off [10]. During the process, strong agitation is needed to ensure a homogeneous suspension and to increase the possibility of bubble-particle collisions [11]. *Fig. 1* shows a schematic drawing of the flotation process.
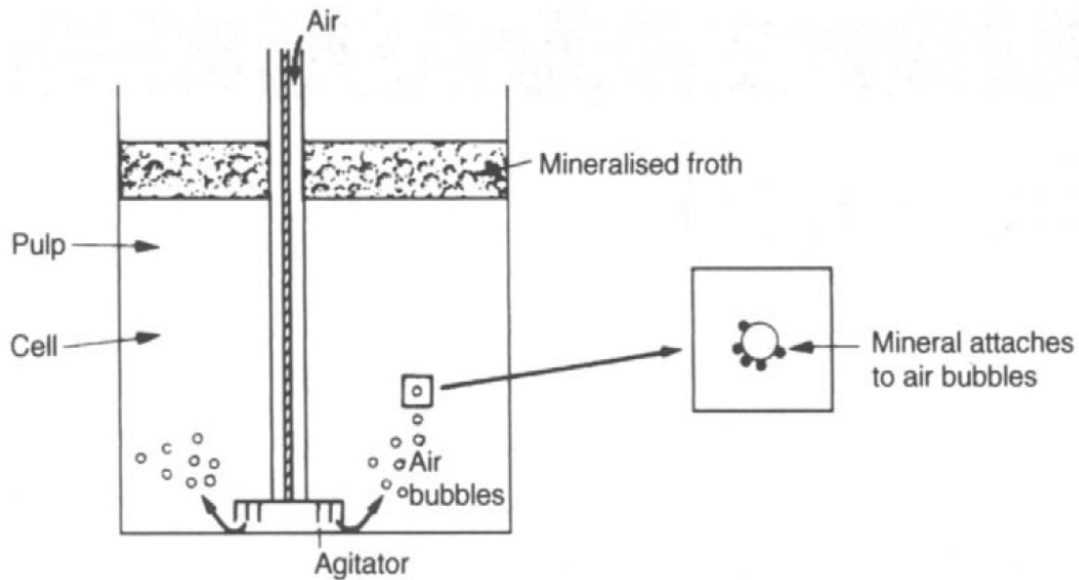
Figure 1: The flotation process [10].

As *Fig. 1* shows, the main mechanism of separation in flotation are the solid-gas interactions that arise from the *hydrophobicity* of the target minerals, and that ultimately leads to the formation of the froth. This process is called true flotation, and it is the basis of most of the industrial flotation processing. [10][12]

Separation can also occur via two other mechanisms called entrainment and entrapment. These phenomena are unwanted due to their lack of selectivity, and measures are often taken to minimize them. All three separation mechanisms are listed below. [10]

1) True flotation: the attachment of a solid particle on to the surface of an air bubble – selective.

2) Entrainment: the separation of a particle suspended in the water phase of the froth – non-selective.

3) Entrapment: the separation of a particle that is physically trapped in between other particles that are truly floated – non-selective.

2.2 The Grade-Recovery Curve

The mineral separation via flotation can never achieve a 100% efficiency. This physical limitation is illustrated in a process-specific grade-recovery curve - an example of which is shown in *Fig. 2.*
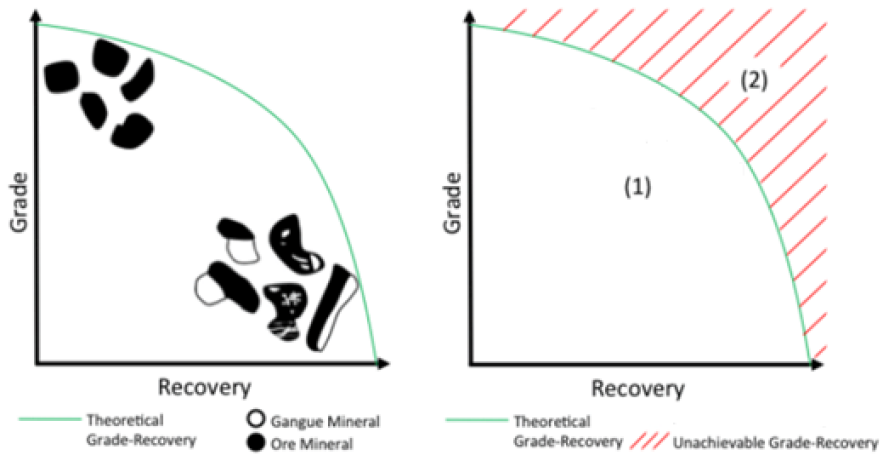
Figure 2: The grade-recovery curve of a flotation system [13].

From *Fig. 2*, we can deduce that a 100% grade (i.e. concentration) can never be obtained with a 100% recovery (i.e. yield) of the valuable mineral. [14] This is due to the non-selective nature of entrainment and entrapment which will always play a role in a flotation system. The theoretical grade-recovery curve is dependent on the particle liberation and size distribution of the minerals, and milling is a common way of trying to improve the grade-recovery performance of a given ore/process [15]. In *Fig. 2*, the green line illustrates the optimal grade-recovery performance of the process. However, in non-optimal conditions, the grade-recovery will not follow this curve. Region (1) represents the achievable values of the grade-recovery – of which the green line only depicts the best performance. Region (2) holds the unachievable values. This region cannot be reached by merely optimizing the chemical environment of the process. To push the green line further to the upright (towards region (2)), milling is always needed. A flotation process should always be optimized to find the best suitable solution for this grade-recovery trade-off [10] [16].

2.3 The Hydrophobic Force

As already stated, for true flotation to happen, the target minerals need to be hydrophobic, which is the single most important characteristic determining the floatability of a given mineral. Hydrophobicity is a natural characteristic of minerals that are covalently bonded and held together by weak van der Waals forces. This chemical set up makes their surfaces non-polar, which hinders their attraction to the water dipoles. Examples of such naturally hydrophobic minerals are coal, diamond, and molybdenite. [10]

One way of determining the hydrophobicity of a given substance, in a three-phase solid-gas-liquid system, is examining the contact angle between the solid/gas interface. This contact angle is a visible representation of the equilibrium of the cohesive and adhesive forces present in the system. *Fig. 3* shows a schematic drawing of these forces. [10][12][17]
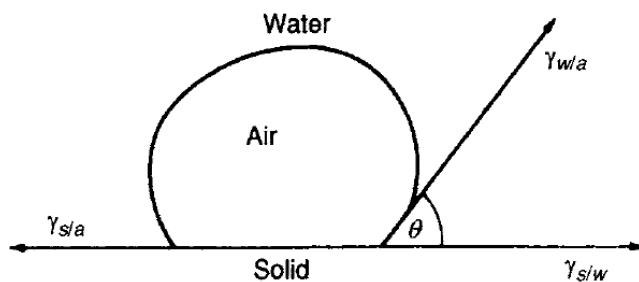
Figure 3: The cohesive and adhesive forces in a solid-air-water system [10].

Mathematically, this same equilibrium of forces can be represented as shown in *Eq. (1)*.

7

$$\gamma_{s/a} = \gamma_{s/w} + \gamma_{w/a} \cos \theta \qquad (1)$$

Where,

$\gamma_{s/a}$ = surface energy between solid/air

$\gamma_{s/w}$ = surface energy between solid/water

$\gamma_{w/a}$ = surface energy between water/air

θ = contact angle between the bubble and the mineral surface

Once a hydrophobic particle has attached on to the bubble surface, a certain amount of energy is needed to disturb the equilibrium, and to break the solid/air interface. This energy is called the work of adhesion ($W_{s/a}$), and it is invested into the creation of the new separate air/water and solid/water interfaces. $W_{s/a}$ can be calculated as shown in *Eq. (2)*.

$$W_{s/a} = \gamma_{s/w} + \gamma_{w/a} - \gamma_{s/a} \qquad (2)$$

Combining *Eq. (1)* with *Eq. (2)* allows us to express the $W_{s/a}$ as a function of the contact angle, as shown in *Eq. (3)*.

$$W_{s/a} = \gamma_{w/a}(1 - \cos \theta) \qquad (3)$$

This result is logical, as it indicates that the larger the contact angle (i.e. hydrophobicity), the more work is needed to disrupt the air/solid interface. [10][12][17]

Only very few minerals possess this hydrophobicity by nature, and thus cannot be floated as is. These *hydrophilic* minerals need to be treated with different surface-active chemicals to achieve the desired hydrophobicity. Nowadays, it is also common to treat naturally hydrophobic minerals to increase their floatability even further. [10] In addition, many other chemicals are also utilized to control a variety of different crucial parameters in the flotation system. The chemicals used to enhance the floatability of ores are discussed in further detail in the next chapter.

2.4   Flotation Reagents

Flotation reagents are a group of chemicals that are utilized to improve the floatability of minerals. These chemicals serve a wide range of purposes, and the effective utilization of them is crucial for all flotation-based mineral processing. Flotation reagents can be roughly divided into four categories which are collectors, depressants, regulators, and frothers [4]. In this chapter, all these groups of chemicals are discussed.

2.4.1   Collectors

Collectors are chemicals that are used in the flotation system to selectively hydrophobize the valuable minerals. They are generally a group of organic compounds that have a heteropolar structure, formed by a non-polar hydrocarbon radical (water-repellant), and a polar group that can react with water. This heteropolarity allows a collector molecule with certain surface-active properties. An illustrative picture of the attachment of a collector onto a mineral surface (the solid-liquid interface) is shown in *Fig. 4*. [10][4]
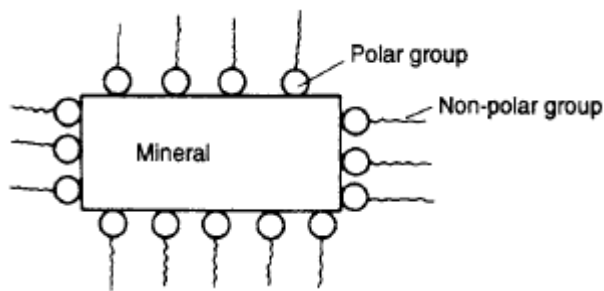
Figure 4: A collector molecule hydrophobizes a hydrophilic mineral [10].

As shown in *Fig. 4*, the hydrophilic mineral is made hydrophobic as the polar head of the collector is adsorbed on the solid-liquid interface, leaving the non-polar tail sticking out. This allows the mineral particles to be attached to the air bubbles, which stabilizes the froth and consequently promotes froth formation.

Collectors of many different compositions have been developed to suit the requirements of a variety of flotation processes. The different types of collectors can be classified based on the functional groups present in the polar regions of the molecule, as presented in *Fig. 5*.
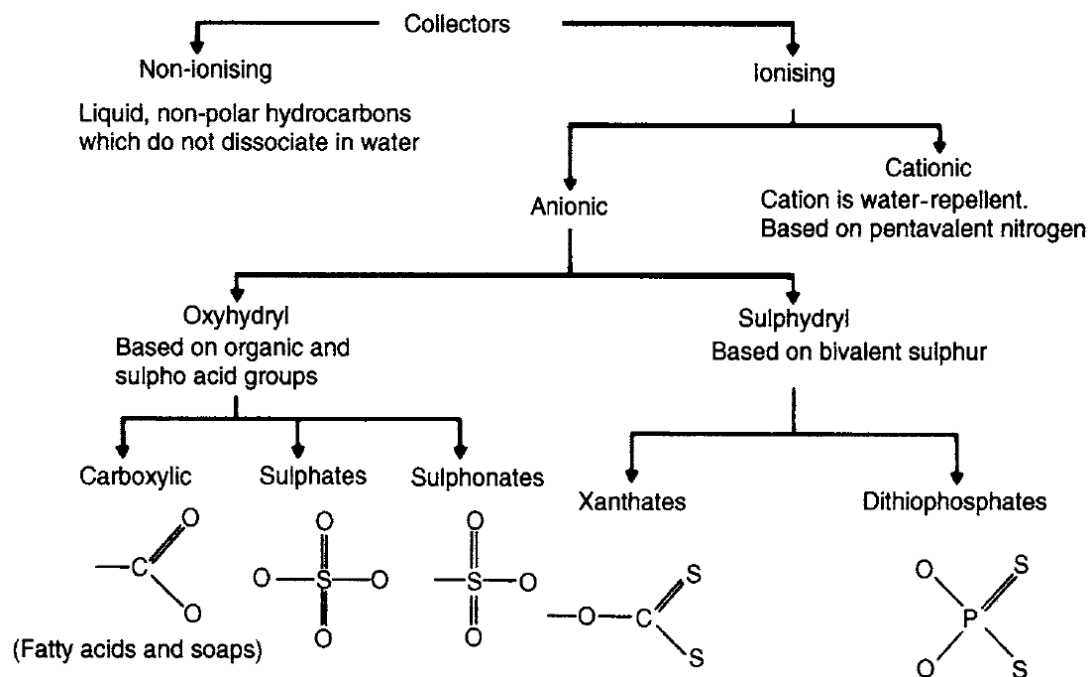
Figure 5: The classification of different collectors [10].

As shown in *Fig. 5,* collectors can be classified based on their ability to dissociate in water, and the type of anion/cation that forms the hydrophilic part of the molecule structure. [4]

2.4.2 Regulators

Regulators are a group of chemicals that are used to control the collector adsorption [4]. These chemicals can be further divided into activators, depressants, and pH regulators.

Activators are used as a pre-processing chemical to promote the subsequent mineral hydrophobization done by a collector. In many cases, simple hydrophobization with a collector is ineffective, due to the hydrophilic nature of the collector products formed

11

in the reactions. To prevent the production of these hydrophilic chemicals, the mineral surface can be treated with a given activator molecule that reacts with it and alters the chemical composition of the surface, so that the hydrophilic collector products cannot be formed. Activators are usually salts that are ionised in solutions. The activating reactions are carried through by these ions. [10]

Depressants are a versatile group of compounds that are used in the flotation process to prevent the hydrophobization of the unwanted minerals and thus promote the selectivity of the collector towards the valuable ones. Most depressants are inorganic molecules, although organic [18] and polymeric [19] ones have been developed as well. The working principles of depressing are complex, and depressants can alter the flotation system in various hard-to-predict ways, including for example the properties of the froth phase. Common depressant molecules used in copper flotation include cyanides (for depressing pyrite) and zinc sulphate (for depressing zinc). [10]

Together with a fine balance of activators and depressants, regulating the pH of the pulp is also important in order to achieve a selective hydrophobization of the valuables. Flotation is mostly carried out in an alkaline medium, the most common pH regulators being sodium carbonate, and calcium hydroxide. [10]

2.4.3 Frothers

Frothers are a group of chemicals that are used in the flotation process to control the properties of the air bubbles in the pulp and froth. The main functions of frothers include reducing the size of the air bubbles, reducing the rising velocity of the bubbles,

stabilizing the froth, and increasing the flotation kinetics [10][11]. The chemical structure of the most common frothers is somewhat similar to those of the collectors. Like collectors, frothers are surface-active agents that are usually composed of a hydrophobic carbon chain, and a hydrophilic polar group, such as carbonyl (C=O), carboxyl (COOH) or hydroxyl (OH) groups [10].

Unsurprisingly, the mechanism of interaction of common frothers also resembles that of the collectors. However, instead of adsorbing onto the mineral surface (the solid-liquid interface), frothers are adsorbed on the bubble surface (the liquid-gas interface). Due to the similarity in the structure of frothers and collectors, some frothers can actually act as collectors, and vice versa [10]. *Fig. 6* shows a schematic drawing of the frother adsorption.
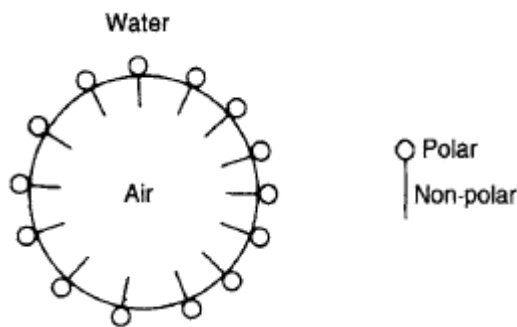
Figure 6: The adsorption of a frother molecule onto the liquid-gas interface [10].

As *Fig. 6* shows, the frother adsorption takes place as the non-polar ends of the molecule orientate towards the gas phase, and the polar ends towards the liquid phase. This surface chemical setup inhibits the coalescence of the bubbles and gives rise to

13

the desired functions of the frothers mentioned earlier. The mechanism of bubble stabilization via frothers is not completely understood [20]. However, the coalescence inhibition is suggested to arise from the hydrogen bonding between the water dipoles and the polar ends of the frother molecules. These bonds, arguably, make it energetically more favourable for the water to not drain from in-between the bubbles (which would ultimately lead to coalescence) and counteracts the thermodynamic drive of lowering the surface area (surface free energy) via bubble coalescence. An additional hypothesis proposes that the lowering of the surface tension (via frother addition) decreases the amount of surface free energy reduced via bubble coalescence and thus reduces the chance of coalescence. [21]

Based on their surface activity, different types of frothers can be roughly divided into weak and strong ones. From an industrial point of view, alcohols are weak frothers, while polyglycols are strong [22]. However, strong frothers are not always favoured over weaker ones, and this classification should be considered somewhat arbitrary. Rather than stating the effectiveness of flotation, the weak-strong-scale corresponds to different froth conditions, and the optimal frother choice is always a matter of the demands of the individual separation process [11]. The froth conditions can refer to, for example, the shallowness/depth of the froth [23], or the amount of water the frother carries. Weak frothers tend to produce shallow and "dry" froths, whereas the froth generated by strong frothers is usually deeper and "wet" [21].

The bubble size of the air phase of the froth is one of the most crucial parameters that determines the flotation efficiency of a given process and, usually, smaller bubbles

tend to enhance the bubble–particle attachment more than larger ones [24]. Therefore, controlling (reducing) the bubble size is one of the most important roles of frothers. [20] Typically, the bubble sizes produced by different frothers are studied in a simplified two-phase system, where only air and liquid is present [11] [25] [26]. The bubble size achieved with a certain frother is a function of the frother concentration, and larger concentrations result in the decrease of the bubble size. However, a given frother can only reduce the bubble size down to a certain point. Also, the size of a bubble population produced with a particular frother concentration will always form a distribution – meaning that bubbles of varying sizes are always present. A common analytical tool used to represent the whole bubble size distribution in a single value is called the Sauter mean diameter (d_{32}). The Sauter mean diameter can be calculated based on a given bubble size distribution as shown in *Eq. (4)* and *Eq. (5)*. [11]

$$d_{32} = \frac{\sum d_{eq}^3}{\sum d_{eq}^2} \tag{4}$$

In *Eq. (4)*, d_{eq} represents the equivalent diameter of the bubble, which can be described as shown in *Eq. (5)*.

$$d_{eq} = \sqrt[3]{d_{max}^2 d_{min}} \tag{5}$$

In *Eq. (5)*, d_{max} and d_{min} are the maximum and minimum diameters of a single bubble in the distribution, respectively. [11] As already mentioned, the bubble size can only be reduced down to a certain point by increasing the frother concentration. The frother-

specific concentration, in which 95% of reduction in the Sauter mean diameter has taken place, is referred to as the critical coalescence concentration (CCC95) value. [26]

The importance of frothers for flotation efficiency has become increasingly evident, and it has been the subject of many studies and reviews [27][28][29]. Recently, pioneering research has been done on innovative new types of frothers. Even the very fundamentals of frother chemistry have been challenged, as macromolecular polymer frothers have been demonstrated to promote some very promising behaviour regarding, especially, the kinetics of the flotation process [9]. In the next chapter, a general review of cellulose and cellulose-based chemicals is made, and one in particular (namely, hydroxypropyl methylcellulose) is studied for its applicability as a flotation frother. Chapter 3.3.3 continues with the theory of macromolecular frothers.

3   Cellulose & Cellulose Derivatives: Case HPMC as a Flotation Frother

This chapter discusses cellulose, cellulose derivatives (especially hydroxypropyl methylcellulose), and the application of cellulose-based chemicals as foaming agents and flotation frothers. First, the structure and properties of natural cellulose are introduced. From there on, the text introduces cellulose derivatives, presenting structural characteristics, properties, and applications. Finally, a deeper insight is given to hydroxypropyl methyl cellulose, and its possible utilization as a flotation frother is discussed.

3.1 Structure & Properties of Natural Cellulose

Cellulose [$(C_6H_{10}O_5)_n$, where n=degree of polymerization] is a linear biopolymer that is comprised of covalently bonded glucose units (pyranose rings/anhydroglucose units). In its structure, two glucose molecules are bonded by β-(l-4)-glycosidic bonds, forming the fundamental unit of cellulose known as cellobiose [30]. The molecular structure of cellobiose is shown in *Fig. 7*.
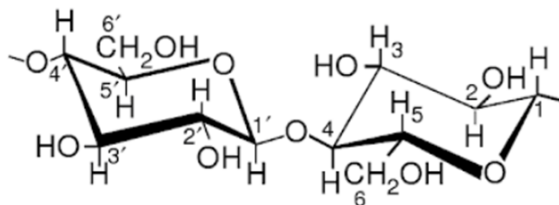
Figure 7: The cellobiose structure [7].

As *Fig. 7* shows, the cellobiose structure is formed as the equatorial OH group reacts to form an ether bond between carbons C4 and C1' of the individual glucose molecules. [30] To minimize the free energy of the system, the pyranose rings all adopt the favorable $^4C_1$ chair conformation [31]. This structure then repeats several times, forming the cellulose polymer, illustrated in *Fig. 8*.
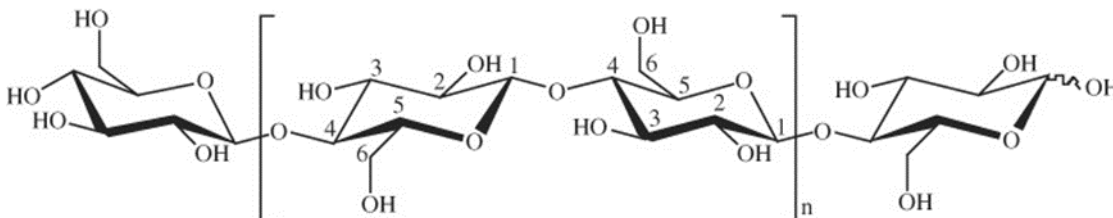
Figure 8: The steric configuration of natural cellulose [32].

The pyranose rings in the opposite ends of the cellulose chain have slightly altered compositions (with regards to each other and the glucose molecules in the chain) and, consequently, they show different chemical behaviors. As *Fig. 8* shows, the right end of the molecule contains an unsubstituted hemiacetal in the C1 carbon, which gives rise to reducing properties. The left end, on the other hand, has an additional hydroxyl group attached in the C4 carbon, and is non-reducing. [31] Furthermore, in *Fig. 8*, the chain length *n*, also known as the degree of polymerization (DP), is a measure of the average amount of monomer units per a cellulose molecule.

On a macromolecular scale, cellulose forms crystalline structures, existing in four known polymorphs (Cellulose I, II, III, and IV). Natural cellulose exists in the cellulose I form, which can be further divided into cellulose Iα and Iβ (Iβ more common) based on the packing pattern in the lattice [30]. The crystallizing tendency of cellulose is due to the intra- and intermolecular hydrogen bonding between the oxygen and hydrogen atoms located in the three hydroxyl groups that each individual pyranose ring hosts. The hydrogen bonding network of the natural Iβ cellulose is shown in *Fig. 9* [33].
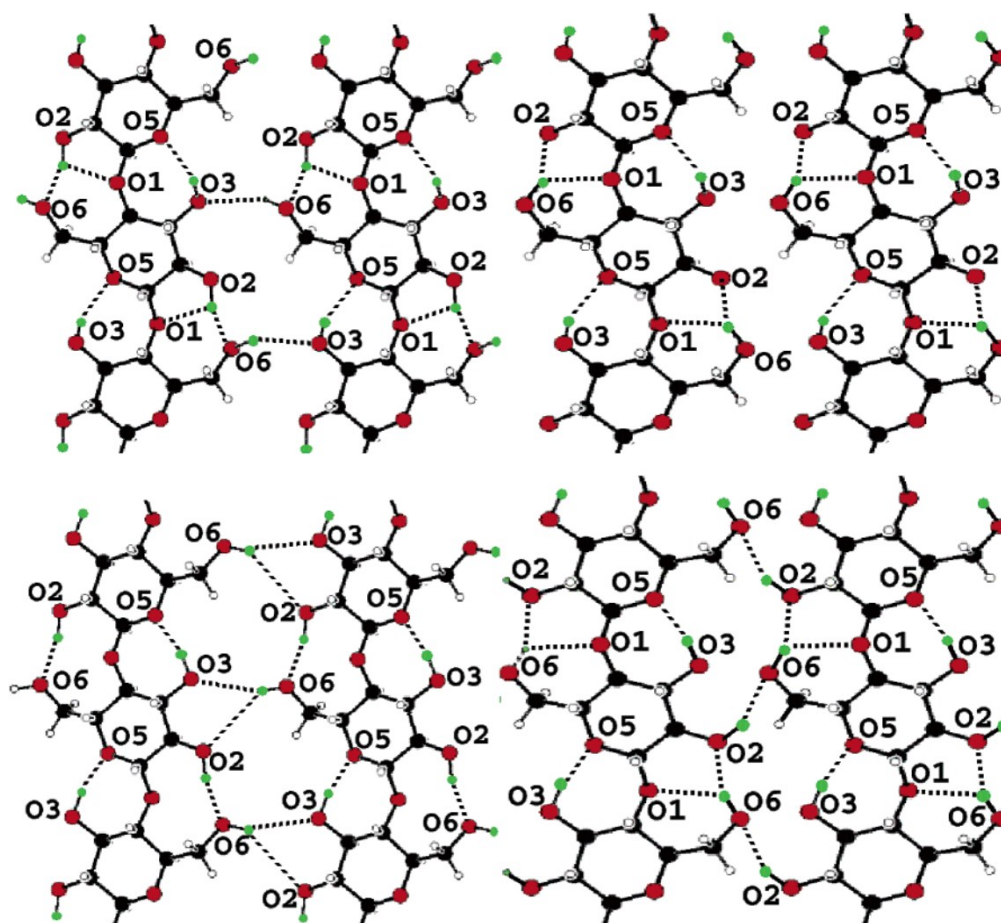
Figure 9: The hydrogen bonding in the top and bottom sheets of the natural cellulose Iβ-structure. Carbon, oxygen, hydrogen, and deuterium atoms are represented by black, red, white, and green spheres, respectively. The cellulose sample has been deuterated only for characterizational reasons, and this same hydrogen bonding network is present also in the natural (non-deuterated) cellulose [33].

In natural cellulose, these stabilized sheets, visualized in *Fig. 9*, organize themselves into a lattice, in either the Iα or Iβ structure. Iα has a triclinic unit cell containing one cellulose chain, whereas the more common Iβ has a monoclinic unit cell containing two parallel cellulose sheets. The space group of cellulose Iβ is $P2_1$, and the lattice

parameters are a = 7.784 Å, b = 8.201 Å, c = 10.38 Å, and γ = 96.5°. [33] The crystal

structure of cellulose Iβ is more precisely visualized in *Fig. 10*, *11*, and *12*.
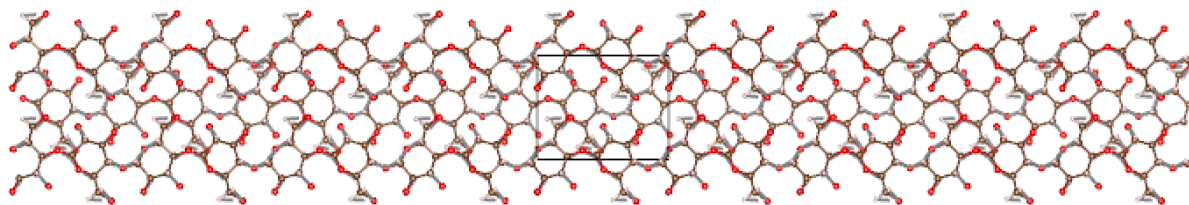
Figure 10: The crystal structure of cellulose Iß visualized from the a-direction (along

the x-axis) [34].
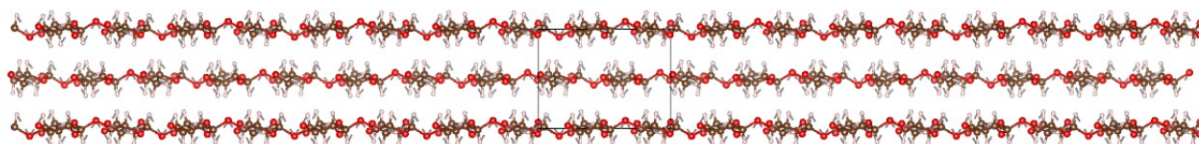
Figure 11: The crystal structure of cellulose Iß visualized from the b-direction (along

the y-axis) [34].
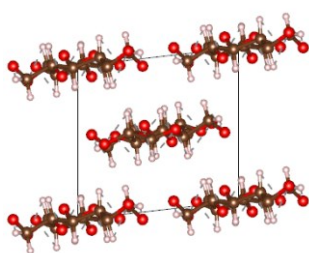
Figure 12: The crystal structure of cellulose Iß visualized from the c-direction (along

the z-axis) [34].

This structure is responsible for many of the fascinating properties of cellulose,

including rigidity, biodegradability, hydrophilicity, [30] and insolubility to most

solvents [35]. However, for some applications, not all these properties are desirable. For example, in the case of flotation frothers, solubility to water is absolutely necessary. In order to be able to utilize cellulose in these cases, its physical properties need to be tailored to properly suit the application.

One method of altering the physical properties of cellulose is modifying it chemically. As shown earlier, in the natural form of cellulose, each anhydroglucose unit hosts three OH-groups (*Fig. 8*), which can react and alter the chemical composition of the molecule [36]. These types of modified cellulose structures are known as cellulose derivatives. Cellulose derivatives, and particularly one known as hydroxypropyl methylcellulose, are discussed in depth in the upcoming chapters.

3.2   Cellulose Derivatives

Cellulose derivatives (CDs) are a group of chemicals, in which the chemical composition of the monomer units (pyranose rings) has been altered. This chemical modification allows the physical properties of CDs to be tailored and makes them suitable for a variety of applications – in which unmodified cellulose fails to perform [7] [31]. This chapter discusses the basics of polymer derivatives, general classification of CDs, cellulose ethers and -esters, and finally makes a deeper look into hydroxypropyl methylcellulose (HPMC), presenting its synthesis and structure, applications, and theory behind its possible utilization as a flotation frother.

3.2.1 Degree of Polymerization, Degree of Substitution, and Molar Substitution

The properties of cellulose derivatives (and other polymer derivatives) are strongly dependent on a few key parameters, which are the degree of polymerization (DP), the degree of substitution (DS), and the molar substitution (MS). Molecular weight is also a useful and important measure, but since it can be derived from the DP and MS [37], it is not discussed here.

The degree of polymerization is a measure of the average amount of monomer units linked in the polymer structure [37], and it can be considered as the chain length of the polymer. Concerning cellulose, the value of DP is heavily dependent on the natural source of the molecule. Typical DP values (in nature) range between 1000-10 000 [32], but the value drops as the molecule is processed into some of its derivatives (typical DP of processed cellulose 100-1000) [38]. Some DP averages of different natural cellulose sources are listed in *Table 1*.

Table 1: Average DP values of different natural cellulose sources [32].

Species	Degree of Polymerization
Cotton	10 000
White birch	5500
White spruce	4000
Eucalyptus regnans	1510

The DP can be used to describe both natural and derivatized cellulose. To further specify the characteristics of a given cellulose derivative, information about the quality, quantity, and position of the substituent molecules is needed as well.

The degree of substitution (DS) measures the average amounts of substituted positions per anhydroglucose unit [39]. As stated earlier, each anhydroglucose unit in the cellulose backbone has three OH groups that are available and can react with substituents. Therefore, the average amount of reacted OH groups (per anhydroglucose unit) is what the DS value represents. Since (regarding cellulose) the maximum amount of substituted positions per each linked glucose molecule is 3, the value of DS is a number between 0 and 3. The DS can also be expressed in percentages (where 3 = 100 %). *Fig. 13* and *Fig. 14* illustrate two different cellulose derivatives, with DS values of 2.0 and 1.0, respectively.
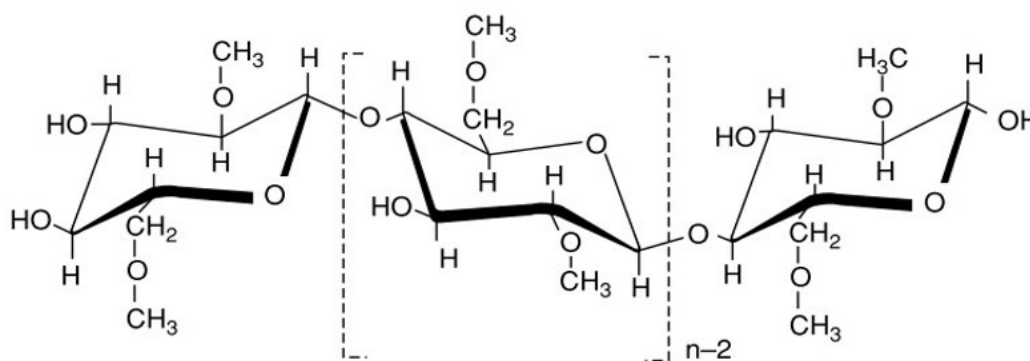
Figure 13: Methyl cellulose with a DS of 2.0. On average, each anhydroglucose ring hosts two side chains [40].
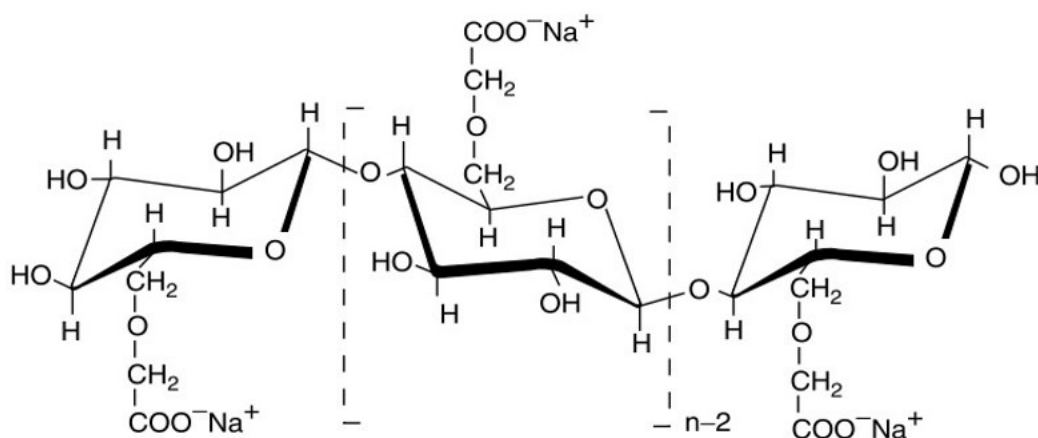
Figure 14: Carboxymethyl cellulose with a DS of 1.0. On average, each anhydroglucose ring hosts one side chain [40].

The molar substitution (MS), on the other hand, measures the average amount (moles) of substituents per anhydroglucose ring [41]. Sometimes, in addition to the OH groups of the anhydroglucose units, the substituents can also react with an already substituted position, initializing side chain growth. In these cases, there is competition between a simple substitution and chain extension. Thus, MS ≥ DS. *Fig. 15* illustrates a hydroxypropyl cellulose molecule with a MS of 2.0.
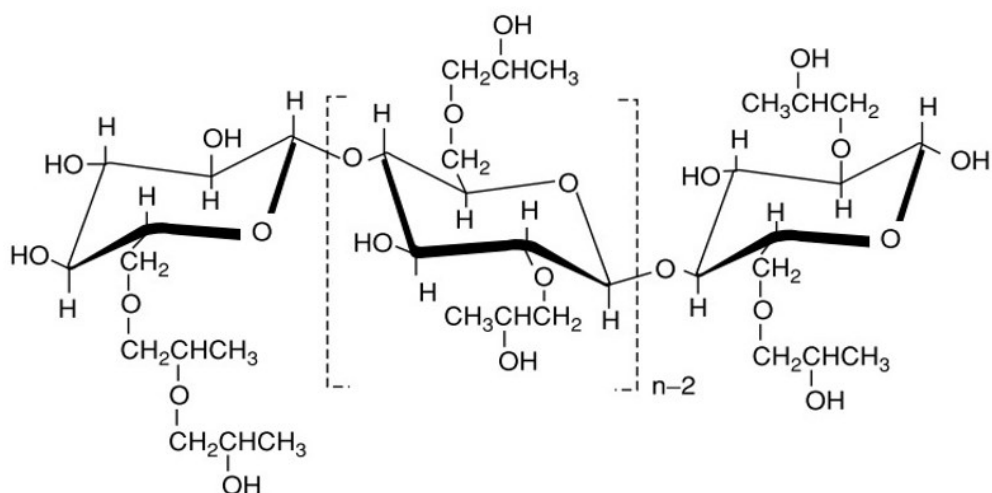
Figure 15: Hydroxypropyl cellulose with a MS of 2.0. On average, each anhydroglucose ring hosts two moles of substituent molecules [40].

In *Fig.* 15, on average, two substitute molecules are attached on each anhydroglucose unit. However, in the left-hand terminal group of the molecule, both hydroxypropyl groups are attached on the same position in the cellulose backbone. This means that, while the MS is clearly 2.0, the DS of the molecule is actually little less than 2. In the upcoming chapter, the general basis of CD classification is discussed.

3.2.2 General Classification

CDs are usually classified either by their physical properties, or their chemical composition. A common physical base of classification is solubility to water, since solubility is often a key parameter regarding the applicability of a given CD. Other useful physical parameters of classification include electrolytic dissociation, and molecular charge (ionic/nonionic). [42] *Table 2* lists some common CDs along with their water solubility status.

Table 2: Common cellulose derivatives listed based on their solubility [42].

Soluble	Insoluble
Cellulose Acetate (low DS) [43]	Cellulose Acetate (high DS) [43]
Hydroxypropyl Methylcellulose (HPMC)	Ethyl Cellulose
Hydroxyethyl Cellulose	Cellulose Acetate Phthalate
Hydroxymethyl Cellulose	HPMC Phthalate

As *Table 2* shows, the DS (also DP and MS) value of the molecule can have a dramatic effect on the physical properties of the chemical. For example, cellulose acetate is water soluble with lower DS values (DS close to 1), whereas higher DS makes it water insoluble (DS close to 3) [43]. In these cases, the properties-based classification can fall short. Therefore, classifying CDs based on their chemical composition is by far more common. This division is done based on the nature of the chemical modification of the pyranose rings or, more formally, the types of functional groups introduced in the substitutions. Two of the most common types of CDs are cellulose ethers and cellulose esters [44]. *Table 3* below lists some of the most common CDs in both of these categories.

Table 3: Common cellulose derivatives listed based on their chemical nature [42].

Cellulose Ethers	Cellulose Esters
Methylcellulose	Cellulose Acetate
Hydroxyethyl Cellulose	Cellulose Nitrate
Carboxymethyl Cellulose	Cellulose Acetate Phthalate
HPMC	HPMC Phthalate

Cellulose ethers and cellulose esters are viewed more thoroughly in the next chapter.

3.2.3 Cellulose Esters

Cellulose esters (CESs) are a group of CDs, in which the hydroxyl groups of the cellulose backbone have been partially or fully replaced with ester structures. CESs are a diverse group of chemicals that perform a variety of functions and have applications in different fields of study. Based on the chemistry of the substituent groups, CESs can be further divided into organic and inorganic ones [45].

Inorganic CESs contain all esterified CDs, in which the oxygen atoms in the cellulose backbone are linked to a non-carbon atom in the substitution group. Examples of such chemicals are cellulose nitrate (nitrocellulose), cellulose sulfate, and cellulose phosphate [45]. Inorganic CESs are often prepared by reacting cellulose with a strong acid, or a combination of acids. For example, in the production of nitrocellulose, a mixture of HNO_3, H_2SO_4, and water is used [46]. This reaction is shown in reaction equation (1).

$$HNO_3 + (C_6H_{10}O_5)_n \xrightarrow{H_2SO_4} C_6H_7(NO)_2O_5 + 3\ H_2O \tag{1}$$
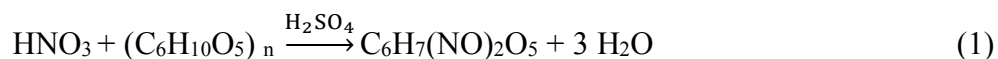
In this reaction, shown in *Eq. (1)*, sulfuric acid catalyzes the formation of a nitronium ion, after which a first order electrophilic substitution of the cellulosic hydroxyl groups follows [46]. The obtained nitrocellulose structure is visualized in its general form in *Fig. 16*.
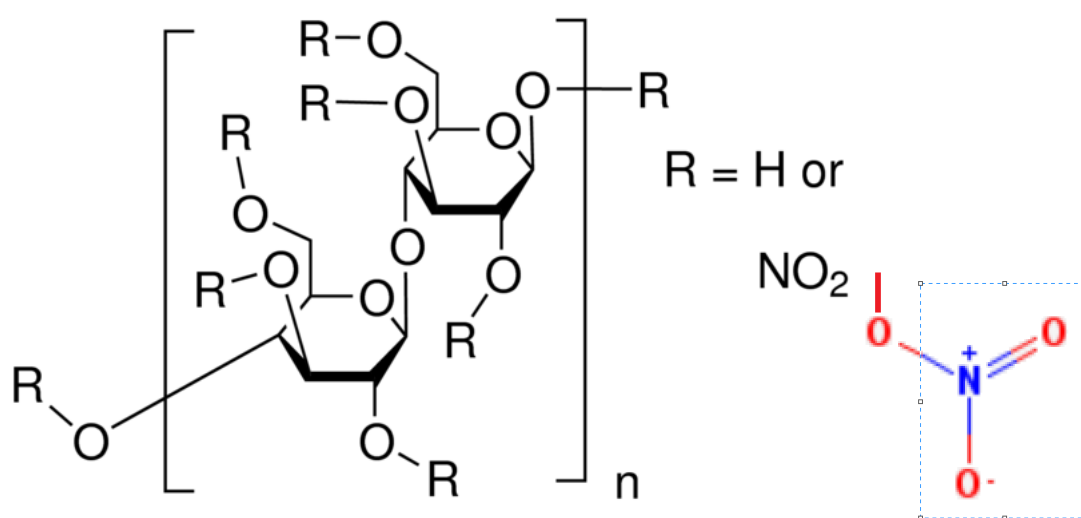
Figure 16: The general formula of cellulose nitrate and the nitrate ester group visualized (the substituted NO₂ in the blue box) [47].

As *Fig. 16* shows, in nitrocellulose, some (or all) of the hydroxyl groups of the cellulose backbone have reacted and formed a nitrate ester group. The structure of the substituted NO_2 group is more precisely visualized on the bottom-right side of *Fig. 16* in the blue box. The oxygen atom outside the blue box is cellulosic. In unsubstituted positions, the OH group remains intact – in which case R=H. The amount of substituted positions is indicated in the DS value of a given commercial nitrocellulose chemical.

Nitrocellulose is the most commercially valuable inorganic CES, and its applications include coatings, adhesives, membranes, pharmaceuticals, and explosives, among others. Other inorganic CESs are used for example in flame retardants (cellulose phosphate), and ion exchange applications (both cellulose sulfate and -phosphate) [45].

Organic CESs, on the other hand, comprise of all esterified CDs in which the cellulosic oxygen atoms are bonded to carbon atoms in the substituents. Examples of such materials include cellulose acetate, cellulose propionate, and cellulose acetate butyrate [48].

Organic CESs are synthesized in reactions involving cellulose and organic acids, anhydrides, or acid chlorides. Nearly any organic acid can be utilized, although CESs of acids involving more than four carbon atoms have been commercially less successful [49]. For example, cellulose acetate, which is the most commercially utilized organic CES [43], is conventionally produced by reacting wood pulp with acetic anhydride and acetic acid (in the presence of sulfuric acid) [50]. By this method, the fully substituted cellulose triacetate (DS=3) is formed, which can subsequently be hydrolyzed to obtain the desired DS value [51]. Various other synthesis methods have been reported in the literature as well [52] [53] [54]. The general structure of cellulose acetate is visualized in *Fig. 17*.
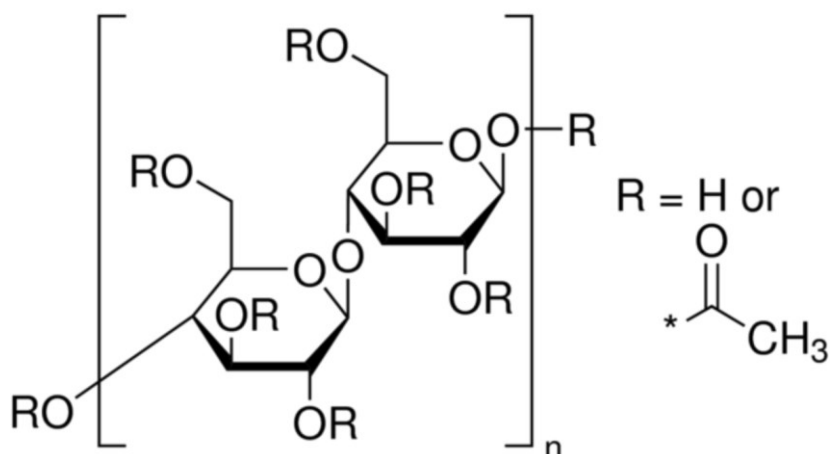
Figure 17: The general structure of cellulose acetate [55].

As *Fig. 17* shows, in cellulose acetate, some (or all) of the hydroxyl groups of the cellulose backbone have reacted and formed an acetate ester group. In unsubstituted positions, the OH group remains intact – in which case R=H. The amount of substituted positions is indicated in the DS value of a given commercial cellulose acetate chemical.

Organic CESs have found use in a variety of applications, including coatings, optical films, composites, biodegradable plastics, controlled release, [48] and medical treatment [56]. Many of these applications overlap with those of the inorganic CESs and, in some of cases, organic CESs (such as cellulose acetate) have been used to successfully replace their inorganic counterparts that host some undesirable properties – example of which would be the historic case of cellulose acetate film replacing the flammable nitrate film [57].

In the next chapter, the theoretical review proceeds to present the other main group of CDs – cellulose ethers. However, hydroxypropyl methylcellulose will be excluded from this chapter, as it will be reviewed more in depth in the upcoming chapter 3.3.

3.2.4 Cellulose Ethers

Cellulose ethers (CETs) are a group of CDs, in which the hydroxyl groups of the cellulose backbone have been partially or fully replaced with ether structures. These derivative chemicals were first commercialized in the beginning of the 20th century, and since then, many different products with varying properties have been developed for commercial use [58]. Although the properties of CETs are diverse, on general basis their characteristics usually involve high chemical stability, solubility, and toxicological innocuousness [6].

CETs are produced from natural cellulose in a two-step process that includes an activation stage, and a subsequent etherification stage [59]. In these reactions, various etherification agents can be utilized, depending on specific CET that is being synthesized – although the process in general is similar for all CETs. There are two main types of industrial etherification processes – one in which sodium hydroxide is consumed, and one that is catalyzed by sodium hydroxide [58]. As an example, the NaOH-consuming synthesis of methylcellulose is shown in reaction equations (2) and (3) [60]. This process is known as the Williamson ether synthesis [59].

$$R - OH + NaOH \longrightarrow R - ONa + H_2O \tag{2}$$

$$R - ONa + ClCH_3 \longrightarrow R - O - CH3 + NaCl \tag{3}$$
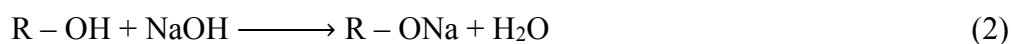
In *Eq. (2)* and *(3)*, R represents an anhydroglucose radical (the cellulose backbone). *Eq. (2)* first shows the activation stage of the synthesis. During this step, the hydrogen

bonding network (*Fig. 9*) is partially or fully disturbed, by reacting cellulose with sodium hydroxide to produce alkali cellulose (RONa) and water. By breaking up the hydrogen bonds of the crystallized cellulose, these newly produced ONa-groups open the structure up for further reactions. During the second stage, shown in *Eq. (3)*, an etherification agent is added, and the final structure of the CET is formed. In the case of methylcellulose, the etherification agent used is chloromethane, and the final products obtained are methylcellulose and sodium chloride [59].

CETs are categorized based on the chemistry of the substituent groups that, together with the DS and MS values, has a vast effect on the properties and applicability of any given CET chemical [58]. Applications of CETs include thickening, binding, water retention [61], and foam and emulsion stabilizers (particularly in the food industry) [62]. *Fig. 18* shows a conceptual visualization of the structures of some of the most common commercial CETs.
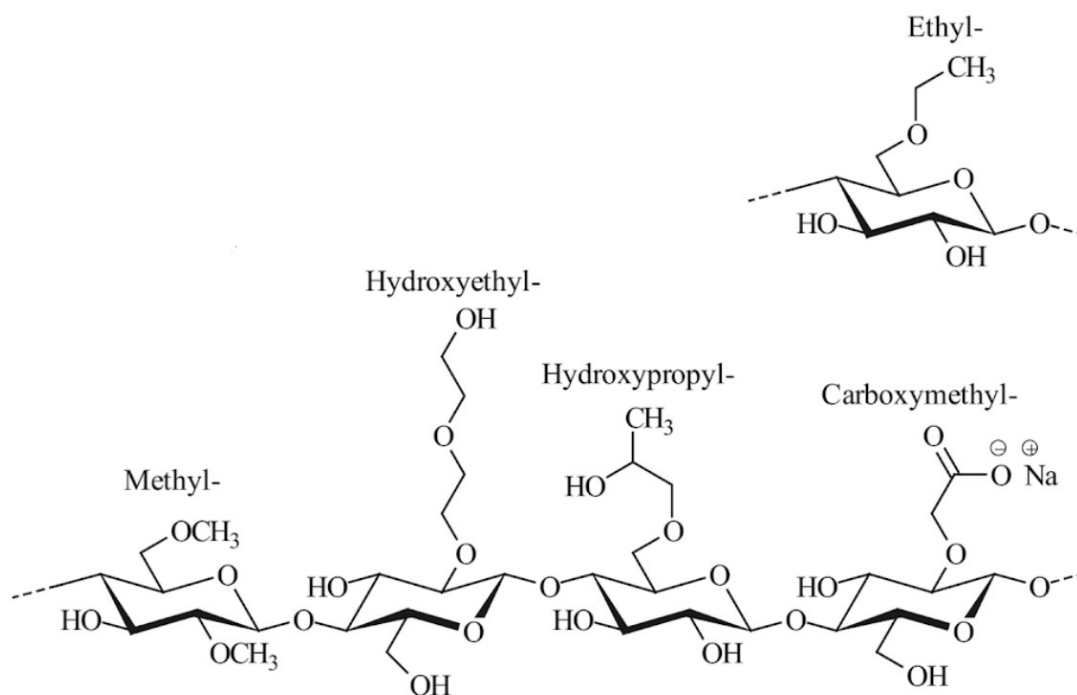
Figure 18: A schematic visualization of a variety of commercialized cellulose ethers [63].

An interesting aspect of cellulose ethers is that they can be synthesized to contain more than one of the derivative groups presented in *Fig. 18* – forming so called mixed-ether structures. Examples of such chemicals include ethyl hydroxyethyl cellulose, hydroxyethyl methylcellulose, and hydroxypropyl methylcellulose (HPMC). These chemicals are well established in the industry, and have found use especially in technical applications [58]. The next chapter discusses HPMC, and particularly its usage in the context of flotation.

3.3   HPMC & Its Utilization in the Context of Flotation

Hydroxypropyl methylcellulose (hypromellose, HPMC) is a mixed ether CD (copolymer of cellulose) that has been synthesized to contain both hydroxypropyl and

methyl functional groups. This chapter describes the synthesis and structure of HPMC, presents its properties and industrial applications, and makes a review of its applicability in the context of flotation.

3.3.1 Synthesis & Structure

In their book, Klemm et al. describe the synthesis of a variety of mixed hydroxyalkylethers that are based on hydroxypropylcellulose (HPC), and hydroxyethyl cellulose (HEC) [59]. Although they do not specifically mention the synthesis of HPMC, it is here by assumed that the procedure is generally the same for this derivative as well. The HPMC synthesis is presented below based on this assumption.

HPMC can be synthesized in two steps, with the hydroxypropyl-, and the methyl groups introduced separately. During the first step, the hydroxypropylation of conventional cellulose occurs by reacting cellulose with propylene oxide in the presence of NaOH. This reaction results in the formation of HPC, and it is described by reaction equation (4).

$$R - OH + C_3H_6O \xrightarrow{OH^-} R - CH_2 CH (OH) CH_3 \qquad (4)$$

In *Eq. (4)*, R represents the cellulose backbone. NaOH (OH^-) is used only in catalytic amounts for the cleavage of the epoxy ring (in propylene oxide) and, unlike in the Williamson synthesis, it is not consumed. The reactivity of the cellulosic OH groups has been observed to follow the trend $C_6 > C_2 > C_3$, in which the C_n depict the carbon in

which the OH group is attached to (*Fig. 8*). Furthermore, due to the introduction of the secondary OH groups (in the already substituted hydroxypropyl groups), this reaction also results in side chain growth of the polymer, meaning that the MS value increases. The side chain growth has been observed to take place especially in the early stages of the reaction, steadily increasing the MS/DS ratio, until it usually settles down to around 1.5-2.5 (MS/DS). [59]

The second step of the reaction is the methylation of the HPC. This can be done, for example, as shown in reaction *Eq. (2)* and *Eq. (3)*. Again, the methylation can result in the substitution of the still available cellulosic OH groups, or the newly introduced secondary OH groups. The HPMC structure thus obtained is visualized in *Fig. 19*. Literature also suggests, that the synthesis could be done the other way around, with the methyl groups introduced first, followed by the hydroxypropylation [64].
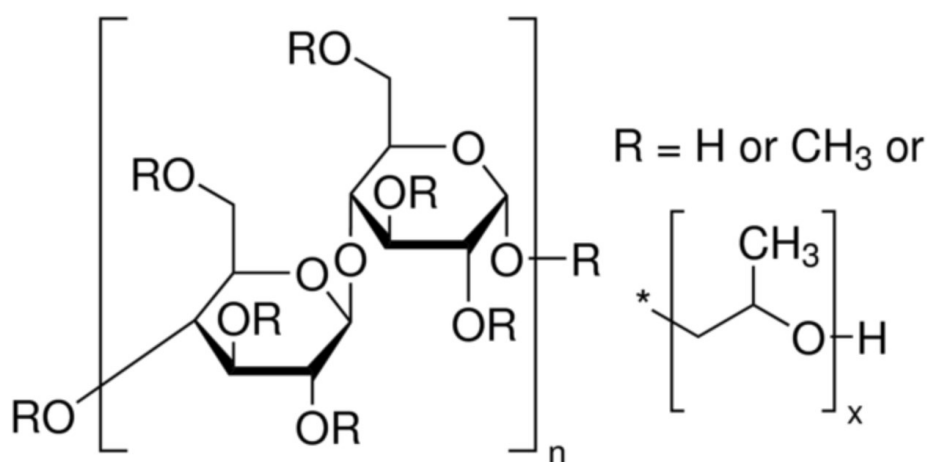
Figure 19: The general structure of HPMC [65].

As *Fig. 19* shows, in HPMC, some (or all) of the hydroxyl groups of the cellulose backbone have reacted and formed either a methoxy or a hydroxypropyl group. Both of these groups need to be present in the molecule in order for it to be recognized as HPMC. In addition, some of the hydroxyl groups may remain unsubstituted (indicated by R=H). Also, in *Fig. 19*, the "x" in the hydroxypropyl group indicates the possibility of the substitution progressing via this position, resulting in side chain growth. The amount of both substituents is indicated in the DS and MS values of a given commercial HPMC chemical. Some vendors may also express the substituent content in weight percentages [65]. Typical commercial HPMC grades have a dry weight percentage of 19-30 % methoxy, and 3-12% hydroxypropyl content [64]. *Table 4* lists four different commercial grades of HPMC, along with the methoxy- and hydroxypropyl contents associated with each grade.

Table 4: *Four examples of different commercial HPMC grades, listed based on their substitution type (methoxy-, and hydroxypropyl contents)* [64].

Substitution Type	Methoxy [wt. %]		Hydroxypropyl [wt. %]	
	Minimum	Maximum	Minimum	Maximum
1828	16.5	20.0	23.0	32.0
2208	19.0	24.0	4.0	12.0
2906	27.0	30.0	4.0	7.5
2910	28.0	30.0	7.0	12.0

3.3.2 Properties & Applications

HPMC, in general, is a non-toxic [66], non-ionic polymer that is odorless, tasteless, inert, viscoelastic, water soluble, and has a white to off-white appearance [64]. Due to the non-toxic nature of HPMC, it has been used extensively in applications that require biocompatibility, namely in the drug [67] and food industries as a gelling and stabilizing agent [68]. Other well-established applications include thickeners, binding agents, emulsifiers [67], water-retainers, lubricants, and film forming agents [64]. The surface-active properties of HPMC are versatile, as the two distinct substituent groups correspond to different chemical behaviors (hydrophobic methyl groups vs. hydrophilic hydroxypropyl groups) [69].

The water solubility status of HPMC is arguably one of the most important characteristics that affect its applicability. This property arises from the etherification of the cellulosic OH groups [70], which disturbs the hydrogen bonding network of natural cellulose (*Fig. 9*) hence lowering the crystallinity of the molecular structure and improving its solubility. The aqueous solutions of HPMC are transparent, stable, and possess a high surface activity. Also, the solubility does not depend on the pH of the solvent. [64] In higher solvent temperatures, HPMC tempts to not dissolve but forms gels instead [64] [66]. The increment of the methoxy content has been observed to increase the solubility, surface activity, and gel point of the polymer. Also, a relation between the solubility and viscosity of the polymer can be observed, as HPMC grades with a lower viscosity are more soluble. Higher molecular weight and chain length (the DP value) of a given HPMC grade tempt to increase the viscosity of its aqueous solution and, consequently, lower its solubility. [64]

In addition, a few important physical properties of HPMC are listed in *Table 5* below.

Table 5: A selection of physical properties of HPMC [64].

Type of HPMC	Physical Property
HPMC	Apparent Density = 0.25-0.7 g/cm^3
HPMC 2% aqueous solution at 20°C	Refractive Index, n_D^{20}= 1.336
HPMC, powdery	Specific Heat, C_p= 1.172 kJ/(kgK)
HPMC, powdery	Thermal Conductivity, k = 0.0484 W/(mK)
HPMC 1% aqueous solution	Specific Gravity = 1.0012
HPMC 5% aqueous solution	Specific Gravity = 1.0117
HPMC 10% aqueous solution	Specific Gravity = 1.0245
HPMC	Static Surface Tension = 42-56 mN/m

The final chapters of this theoretical review discuss the possibility of utilizing HPMC as a frother in the context of flotation, by presenting its interfacial behavior, bubble stabilization potential compared to a commercial frother, and further knowledge regarding the topic.

3.3.3 HPMC as a Surfactant: Interfacial Behavior

The chemistry of HPMC is fundamentally different compered to typical commercial frothers. As mentioned in chapter 2.4.3, conventional frothers are short-chained molecules, with a heteropolar structure that allows them to adsorb on the liquid-gas

interface and stabilize air bubbles in water. The adsorption process (visualized in *Fig. 6*) is well-defined, and the spatial orientation of the adsorbing chemicals (the frother molecules) is always the same. However, in the case of the macromolecular HPMC, the chain length of the polymer is much longer, and there are no simple polar and non-polar ends of the molecule. This makes the adsorption of a polymer frother vastly different compared to a conventional one [71]. *Figure 20* visualizes the adsorption of a macromolecular surfactant – in this case HPMC. In the case of flotation, the interface in question is the liquid-gas interface.
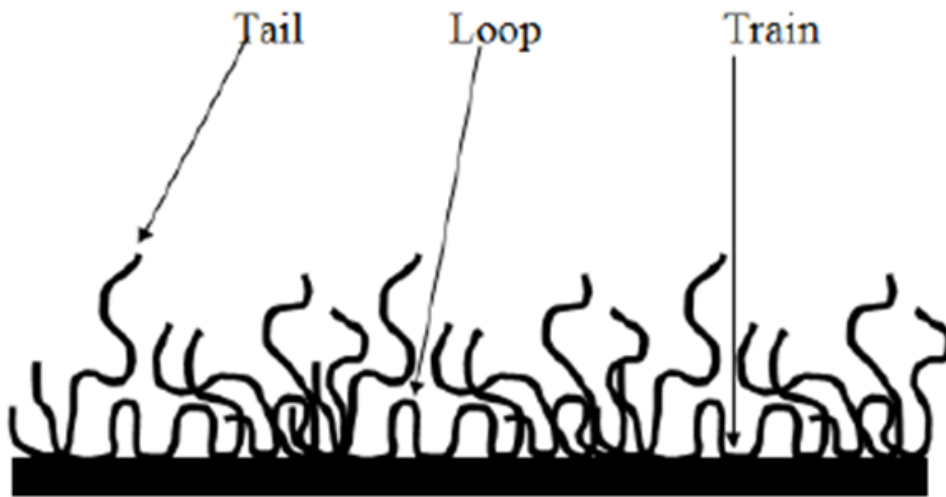
Figure 20: The train-loop-tail model for the adsorption of macromolecular surfactants [71].

As *Fig. 20* shows, the polymer surfactant adsorbs on various locations on the interface, forming a so-called train-loop-tail structure. On the interface, trains are areas in which the surfactant has adsorbed on continuously. Between the trains are the loops, which represent parts of the polymer that are not adsorbed, but still are connected to the

39

interface from both ends. Finally, tails are polymer segments that are connected to the interface from one end only. [71]

The elasticity of the adsorbed polymer layer, together with the ratio of the train, tail, and loop structures, have a vast effect on the stability of the interface and the coalescence prevention [69]. Furthermore, the adsorption of a non-ionic macromolecular frother is a dynamic and complex phenomenon, and the interfacial conformation of the surfactant molecule influences the properties of the interface drastically [72]. The time-dependence of the adsorption process is visualized in *Fig. 21.*
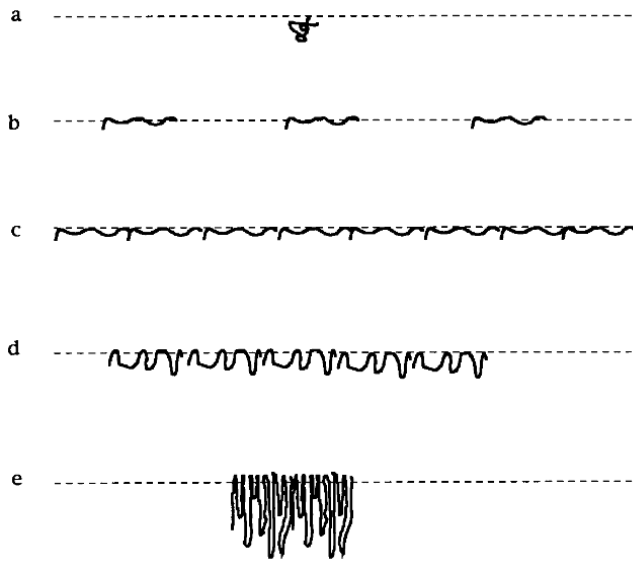
Figure 21: The adsorption process of a non-ionic macromolecular surfactant visualized in distinctive moments in time (t = a, b, c, d, and e) [72].

As *Fig. 21* shows, the adsorption process starts with the diffusion-driven transport of the surfactant molecules from bulk to the interface (t = a). The adsorbed molecules

then start to spread and unfold on the surface (t = b, and c). Finally, the spread-out molecules rearrange into the train-tail-loop segment (t = d). Over time, the orientation of the molecule, and the ratios of the train-tail-loop segments can also change, as the length and quantity of the loops and tails increases (t = e) [72]. At the air-water interface, a drop in the surface tension can be observed, as the loops and tails become the dominating segments [69].

Controlling this adsorption process is one of the main challenges regarding the applicability of HPMC in bubble stabilization. The next chapter discusses the observed bubble stabilization capability of HPMC in further detail.

3.3.4 Bubble Stabilization via HPMC in a Two-Phase Air-Liquid System

The bubble stabilization and the bubble size reducing potential of HPMC have not yet been extensively studied in the literature. However, in the author's research group, pioneering experiments on these topics have been conducted by fellow researchers [9]. The results from these studies are discussed in this chapter.

Fig. 22 and *Fig. 23* show the Sauter mean diameter as a function of frother concentration in pH 5.5 (*Fig. 22*) and pH 10 (*Fig. 23*). The comparison has been done between a commercial frother known as Nasfroth 240 (NF240), and a specific quality of HPMC, hereby referred to as HPMC 40-60. Both frothers have been studied individually (frother concentrations 8-50ppm), and in mixtures with one another. In the mixed-frother experiments, the concentration of one frother has been kept constant

(16ppm), while steadily increasing the concentration of the other (8-30ppm), and vice versa.
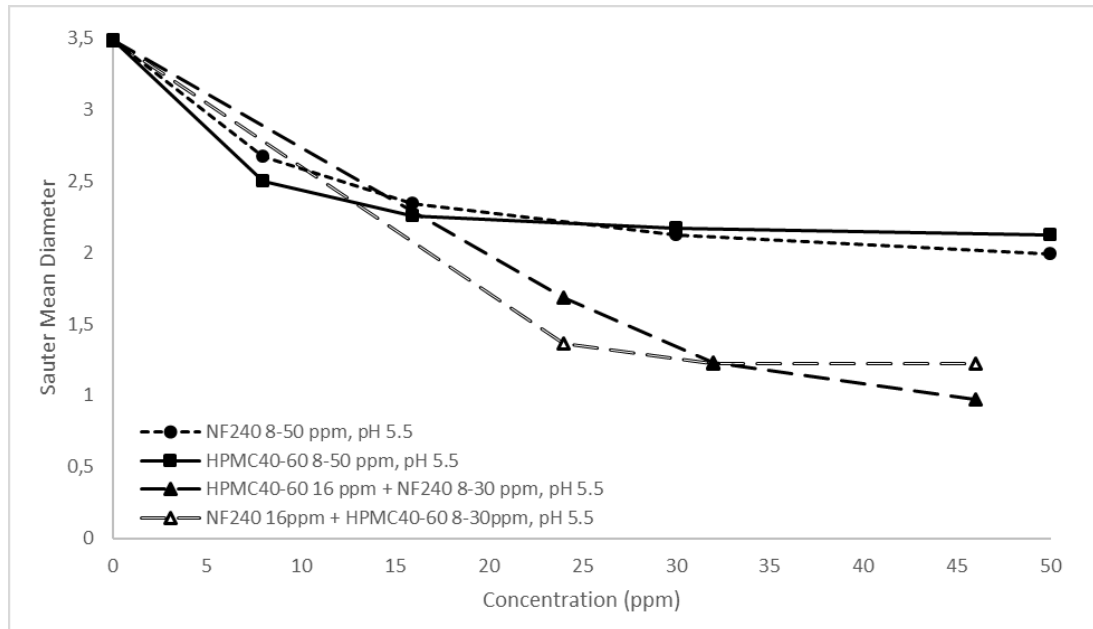
Figure 22: The Sauter mean diameter as a function of the frother concentration in a slightly acidic medium (pH 5.5) [9].
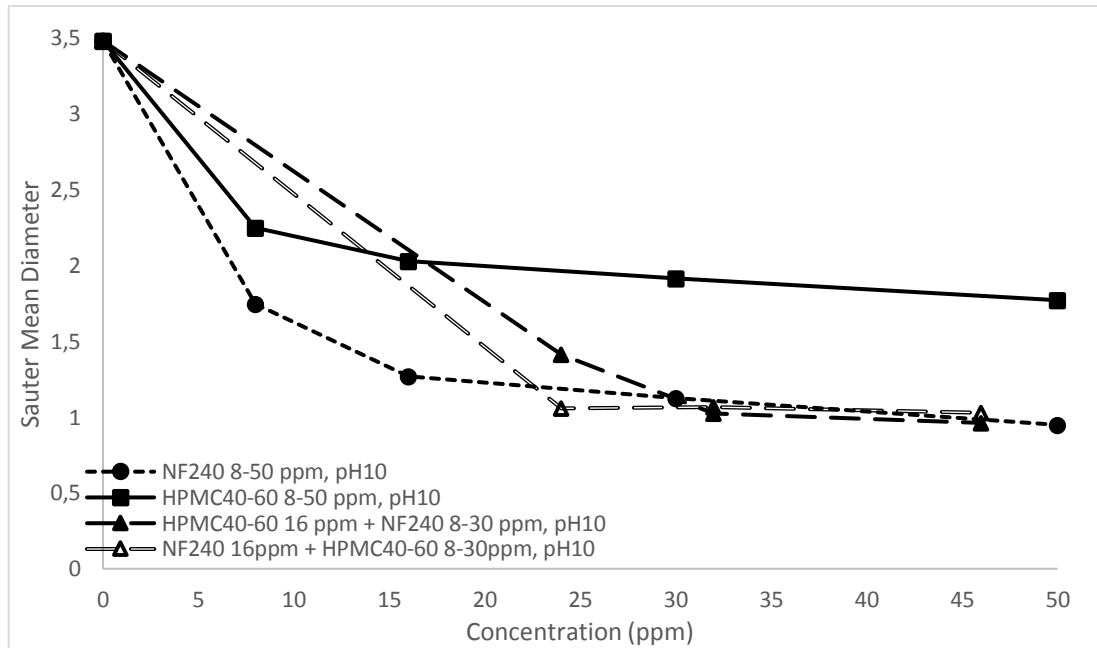
Figure 23: The Sauter mean diameter as a function of the frother concentration in an alkaline medium (pH 10) [9].

These results indicate that the bubble size reducing potential of HPMC 40-60 is well-comparable with the commercial frother in a lower pH environment, whereas in an alkaline medium the commercial frother results in a smaller bubble size. Interestingly, when compared to NF240, both of the mixtures seem to produce much smaller bubbles in pH 5.5. In pH10, the Sauter mean diameter of both mixtures and NF240 seem to approach virtually identical values. As bubble size is an important indicator of the flotation efficiency [24], these results give a reason to believe that HPMC 40-60 would perform similarly to NF240 in a slightly acidic environment, whereas in alkaline medium, the commercial frother would yield better results. However, as flotation is usually carried on in alkaline medium [10], the performance in higher pHs should be considered more relevant. In this case, it looks as though the bubble stabilizing ability of the mixtures (in pH10) is more prominent, compared to pure HPMC 40-60.

When the individual bubble size distributions produced by pure water, NF240, HPMC 40-60, and a mixture (30ppm NF240 + 16ppm HPMC 40-60) are compared, a clear distinction can be made between them. This comparison (in pH 5.5) is done in *Fig. 24*.
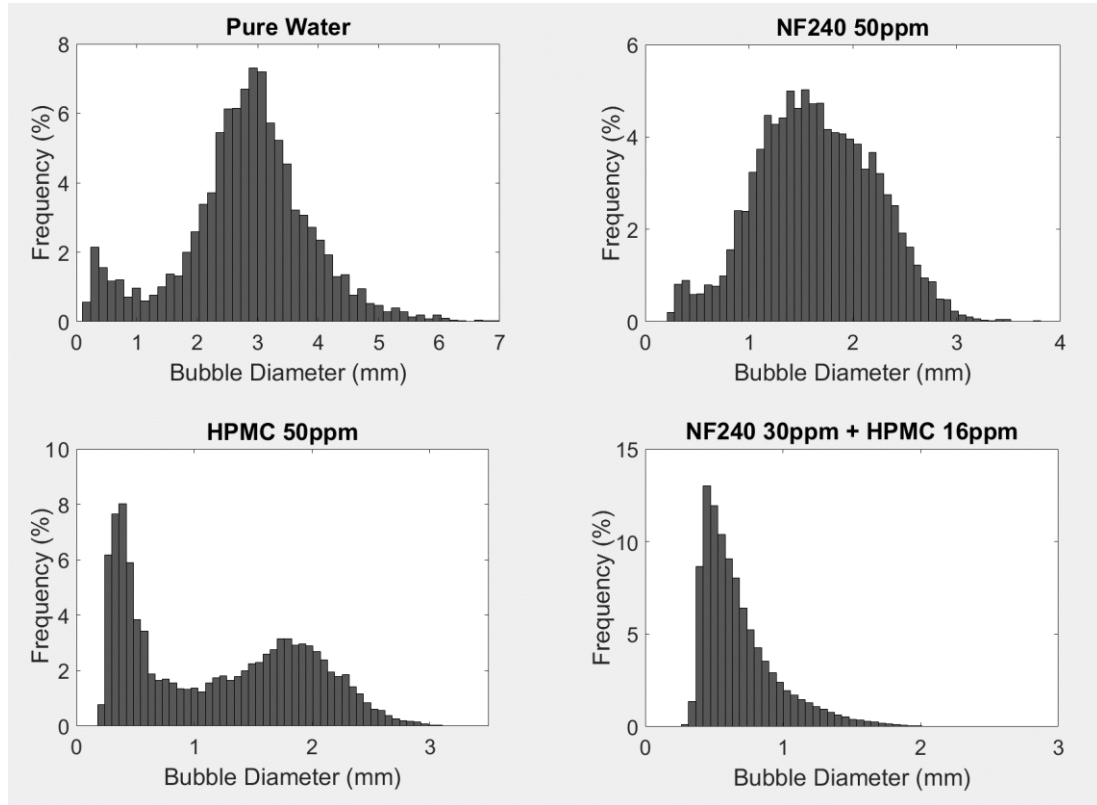
Figure 24: The bubble size distributions of pure water, NF240 (ppm), HPMC 40-60 (50ppm), and a mixture (30ppm NF240 + 16ppm HPMC 40-60) in pH 5.5 [9].

As *Fig. 24* shows, the bi-modal distribution, which is present in the pure water graph and also reported in the literature [26], is conserved with HPMC 40-60. However, HPMC 40-60 is still clearly reducing the bubble size, as the HPMC-stabilized bubble population has been tweaked towards the left side of the graph (smaller bubble size). The bubble population produced by NF240 seem to follow a normal distribution, and a clear reduction in the bubble sizes compared to the pure water can be observed. The

mixture is clearly distinct from all of the other graphs, as it has a very sharp peak at the left (lots of small bubbles), followed by what seems to be a linearly decreasing trend of larger bubbles at first. At a bubble size of ca. 0.7mm, the decreasing trend of the larger bubbles seems to become inversely proportionate. This does not contradict the results shown in *Fig. 22*, as it has been shown, that non-similar bubble size distributions can have the same Sauter mean diameter [11]. Furthermore, research done in the author's department has shown that in higher pHs (pH 10) the bubble size distribution of NF240 resembles that of the mixtures in pH 5.5. This might indicate that mixtures of NF240 and HPMC 40-60 could be utilized in flotation processes that are performed in lower pH environments.

In *Fig. 25*, a closer look on the frother concentration dependency of the bubble size distribution (in the case of HPMC 40-60) has been made.
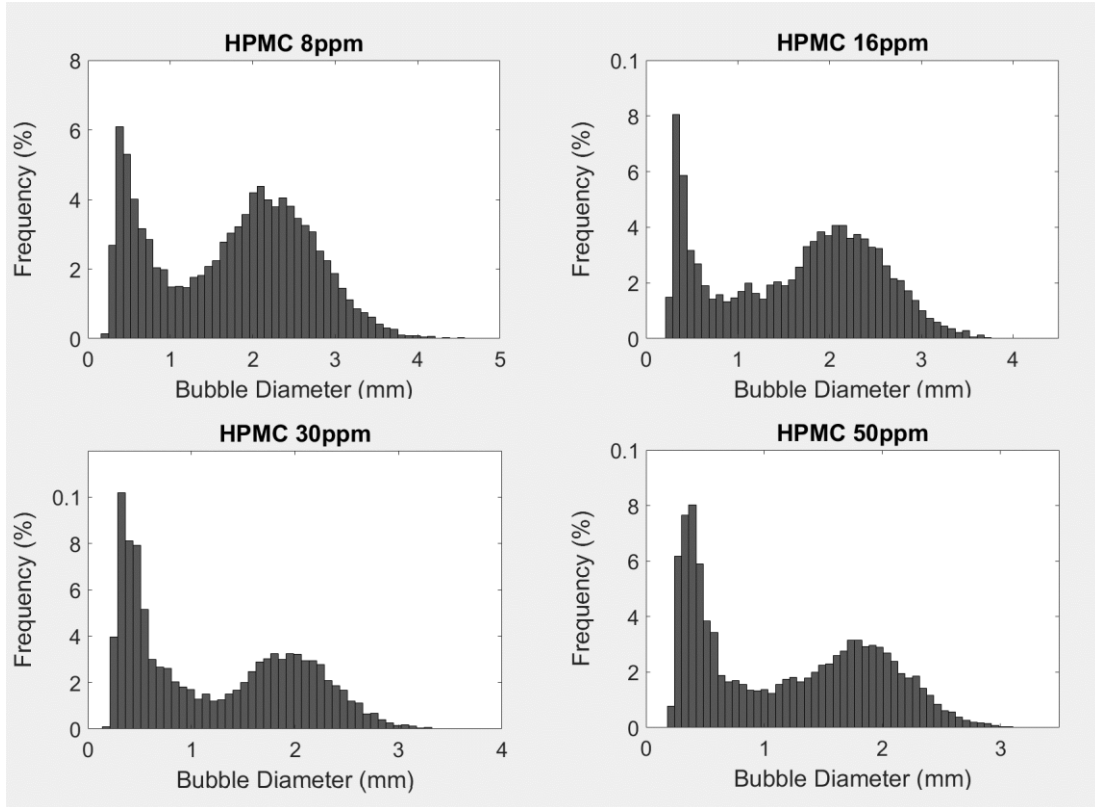
Figure 25: The frother concentration dependency of the bubble size distribution produced by HPMC 40-60 [9].

From *Fig. 25*, it can be seen that the bi-modal bubble size distribution is present in all HPMC 40-60 concentrations. However, even at low concentration (8ppm) the bubble sizes in the population are significantly smaller than in pure water (seen in *Fig. 24*, upper-left). Increasing the HPMC concentration from 8ppm > 16ppm > 30ppm > 50ppm results in a decreasing bubble size, although at higher concentrations the effect is not as noticeable. When, for example, the bubble size distributions with HPMC concentrations of 30ppm and 50ppm are compared, it can already be seen that the large-bubble peak at ca. 2mm is quite stable. Furthermore, in the 50ppm HPMC concentration, the small-bubble peak seems to be widening but not growing taller. The additional HPMC seems to be reducing the size of the bubbles that are already

relatively small, while the larger ones stay somewhat unaffected. All in all, this small-bubble peak can be viewed as evidence for the bubble coalescence prevention of HPMC 40-60, and it is arguably even superior to NF240, when it comes to the stabilization of the smallest bubbles in the population.

3.3.5 Questions to be Answered Regarding the Applicability of HPMC

The performance of HPMC, in the context of flotation, has not yet been studied thoroughly, and consequently many open questions remain. For example, as is known, some frothers may exhibit collector-like properties, meaning that they can adsorb both on the liquid-gas (frother-like behavior), and solid-liquid (collector-like behavior) interfaces [10]. Whether or not this is the case with HPMC is an important question, particularly knowing the sensitivity of flotation to the slightest of changes in the chemical environment. Also, as the molecular structure of HPMC can be tailored, a wide variety of different HPMC grades need to be studied, in order to find the optimal type of molecule for the application of flotation.

4 Experimental Part

4.1 Preparations for the Experiments

A total of four sets of feed ores were used in the flotation tests. In addition, three experiments were carried out with a naturally hydrophilic quartz sample, to determine the amount of non-selective mineral extraction via entrainment. Prior to the flotation experiments, all the feeds were divided into sample bags of ca. 300g using a Retsch rotary sampling machine to ensure a uniform particle size distribution (PSD) in each

bag. For each feed type, water content was measured by weighing the samples wet and after drying in an oven. Each different feed was also test-milled, and particle size analyses (PSAs) were carried out to determine the appropriate milling time for each feed, to keep the PSDs as similar as possible. In some of the PSAs, the samples were also sonicated for three minutes to break any aggregated clusters of particles which would have falsely influenced the PSDs.

4.2   Materials & Methods

4.2.1   Feed Materials

The feeds used for the flotation experiments were Cu-Zn ore from First Quantum Minerals Ltd.'s Pyhäsalmi (Finland) mine, and 99,2% purity quartz from Nilsiä (Finland) ordered from Sibelco Nordic Oy Ab. The different feed materials are listed in *Table 6.*

Table 6: The feed materials for the flotation experiments.

Sample Name	Status
PS Freezedried Ore	Freezedried Pyhäsalmi flotation feed
PS Sieved Ore	Pyhäsalmi ore from the crusher – sieved below 1300μm
PS Crushed Ore	Pyhäsalmi ore from the crusher – the >1300μm fraction left from sieving re-crushed below 1300μm
PS Natural Ore	Pyhäsalmi ore from the crusher – sieved below 3350μm
Nilsiä Quartz	100-600μm SiO_2

As *Table 6* indicates, in addition to the Nilsiä quartz sample, a total of five different Pyhäsalmi ore/tailings materials were used in the flotation experiments. Four of these materials were all, in principle, the same Cu-Zn ore but they varied in their moisture content, processing, and/or PSDs. "PS Freezedried Ore" was a fully pre-processed ore, which was already conditioned, freezedried, and could be used directly as a feed in the Pyhäsalmi flotation circuits. The "PS Sieved Ore", "PS Crushed Ore", and "PS Natural Ore" were ores from the crusher, meaning that they had not been milled to the optimal particle size. During the experiments, laboratory-scale milling was done for each feed batch to get the PSDs of the crushed and the fully pre-processed ores as similar as possible.

4.2.2 Chemicals

The chemicals used in the flotation experiments are listed in *Table 7*.

Table 7: The different chemicals used in the flotation experiments.

Name	Chemical Formula / Acronym	Type
Nasfroth 240	$C_4H_9(OC_2H_4)_3OH$ / NF240	Frother
Hydroxypropyl methylcellulose high MW	HPMC 40-60	Frother
Hydroxypropyl methylcellulose low MW	HPMC 10K	Frother
Sodium Isobutyl Xanthate	$C_5H_9NaOS_2$ / SIBX	Collector
Zinc Sulfate	$ZnSO_4$	Sphalerite Depressant
Sodium Sulfite	Na_2SO_3	Pyrite Depressant
Sodium Hydroxide	NaOH	pH Regulator
Calcium Hydroxide	$Ca(OH)_2$	pH Regulator

The commercial glycol ether frother NF240 was purchased from Nascao International LLC, and the HPMCs were obtained from Sigma-Aldrich (product No.'s H8384 and 423238). According to the distributer, the average molecular weight of HPMC 40-60 was 22 kDa, with a methoxy content of 28-30 wt. %, and a hydroxypropoxyl content of 7-12 wt. %. For the HPMC 10K, these values were 10 000 g/mol, 29 wt. % methoxy, and 7 wt. % propylene oxide, respectively.

4.2.3 Particle Size Analysis Machinery

The PSAs were carried out in an aqueous suspension, using a Malvern Mastersizer 3000 Hydro EV unit shown in *Fig. 26*.

Figure 26: The Malvern Mastersizer 3000 particle size analyzing machine.

During the particle size measurements, abnormalities were monitored with the Malvern Hydrosight unit shown in *Fig. 27*.

Figure 27: The Hydrosight monitoring unit.

4.2.4 Milling Equipment

Samples were weighed using the Precisa XB 6200D laboratory scale, with the precision of 0.1 grams. Milling was done with a laboratory scale ball mill, using a 5.67 L milling container, and a specific set of milling balls with a ball charge of 5.5 kg. The sizes and amounts of different milling balls are listed in Appendix I. The ball mill is presented in *Fig. 28*.

Figure 28: The ball mill used in the experiments.

4.2.5   Flotation Machinery, General Lab Equipment & XRD Machinery

Elga Purelab Option-R 7/15 was used to obtain purified water with a resistivity of 15,0

MΩ. All the experiments were carried out with an Outokumpu batch flotation machine,

in a 1.5 L glass flotation cell. The flotation machine is illustrated in *Fig. 29*.

Figure 29: The Outokumpu batch flotation machine.

For filtration, 0.45 μm filter paper was used, and the samples were dried in a Jouan laboratory hot air oven. To characterize the samples, Oxford Instruments X-Met 5100 X-ray fluorescence (XRF) gun was used. The XRF gun is illustrated in *Fig. 30*.

Figure 30: Oxford Instruments X-Met 5100 XRF gun.

4.3   Experimental Plan

4.3.1   Preliminary Experiments

To develop an acceptable experimental protocol for the flotation of Pyhäsalmi ore, and to screen the behavior of HPMC and other chemicals in our flotation system, a total of 25 preliminary experiments were performed, in which various parameters for Cu-Zn flotation were studied. These 25 experiments can be further divided into three subsets of experiments, based on the studied parameters. The first subset was formed by quartz flotation experiments, the second one by the experiments done under a personal research assignment course (PRA Flota), and the third one by the "Pre-Thesis Flota" experiments. *Table 8* lists all the performed preliminary experiments along with their experimental setups.

Table 8: The experimental plan for the preliminary flotation experiments.

Name	Frother(s) / Concentration(s) [ppm]	Milling Time [min]	pH Control (Chemical Used)	Amount of SIBX [g/t] / ZnSO₄ [g/t]	Feed Material
Quartz Flota 1	NF240 / 50ppm	10	No	None	Nilsiä Quartz
Quartz Flota 2	HPMC 40-60 / 50ppm	10	No	None	Nilsiä Quartz
Quartz Flota 3	NF240 + HPMC 40-60 / 30ppm + 16ppm	10	No	None	Nilsiä Quartz
PRA Flota 1	NF240 / 30ppm	12.5min	pH 10 (NaOH)	70 g/t + 250 g/t	PS Sieved Feed
PRA Flota 4	NF240 / 30ppm	12.5min	pH 10 (NaOH)	None	PS Sieved Feed
PRA Flota 28	NF240 + HPMC 10K / 16ppm + 16ppm	12.5min	pH 10 (NaOH)	None	PS Sieved Feed
PRA Flota 23	HPMC 10K / 30ppm	25min	pH 10 (NaOH)	None	PS Sieved Feed
PRA Flota 13	NF240 + HPMC 40-60 / 16ppm+16ppm	12.5min	pH 10 (NaOH)	70 g/t + 250 g/t	PS Sieved Feed
PRA Flota 26	NF240 + HPMC 10K / 16ppm + 16ppm	25min	pH 10 (NaOH)	70 g/t + 250 g/t	PS Sieved Feed
PRA Flota 22	HPMC 10K / 30ppm	12.5min	pH 10 (NaOH)	None	PS Sieved Feed

Pre-Thesis Flota 1	NF240 / 30ppm	25min	pH 12 (NaOH)	70 g/t + 250 g/t	PS Crushed Ore
Pre-Thesis Flota 2	NF240 / 30ppm	25min	pH 12 (NaOH)	70 g/t + 400 g/t	PS Crushed Ore
Pre-Thesis Flota 3	NF240 / 16ppm	25min	pH 12 (NaOH)	70 g/t + 400 g/t	PS Crushed Ore
Pre-Thesis Flota 4	NF240 / 16ppm	25min	pH 12 (NaOH)	50 g/t + 400 g/t	PS Crushed Ore
Pre-Thesis Flota 5	NF240 / 16ppm	25min	pH 12 (NaOH)	30 g/t + 400 g/t	PS Crushed Ore
Pre-Thesis Flota 6	NF240 / 24ppm	25min	pH 12 (NaOH)	30 g/t + 500 g/t	PS Crushed Ore
Pre-Thesis Flota 7	NF240 / 24ppm	30min	pH 12 (NaOH)	30 g/t + 500 g/t	PS Crushed Ore
Pre-Thesis Flota 8	HPMC 10K / 24ppm	30min	pH 12 (NaOH)	30 g/t + 500 g/t	PS Crushed Ore
Pre-Thesis Flota 9	HPMC 40-60 / 24ppm	30min	pH 12 (NaOH)	30 g/t + 500 g/t	PS Crushed Ore
Pre-Thesis Flota 10	HPMC 40-60/ 24ppm + 10*8ppm	30min	pH 12 (NaOH)	30 g/t + 500 g/t	PS Crushed Ore
Pre-Thesis Flota 11	HPMC 40-60 / 50ppm	10min	pH 10 (NaOH)	50 g/t + 200 g/t	PS Ore Freezedried
Pre-Thesis Flota 12	HPMC 40-60 / 50ppm	10min	pH 12 (NaOH)	50 g/t + 200 g/t	PS Ore Freezedried
Pre-Thesis Flota 13	HPMC 40-60 / 50ppm	5min	pH 12 (NaOH)	30 g/t + 200 g/t	PS Ore Freezedried

Pre-Thesis Flota 14	HPMC 40-60 / 50ppm	5min	pH 12 (NaOH)	30 g/t + 500 g/t	PS Ore Freezedried
Pre-Thesis Flota 15	HPMC 40-60 / 40ppm	5min	pH 12 (NaOH)	30 g/t + 500 g/t	PS Ore Freezedried

As shown in *Table 8*, the first three preliminary experiments (done with the quartz sample) form the first subset of this experimental plan. These tests were carried out to study the effect of entrainment to the mass pull of the subsequent experiments done with the ore. Quartz is a naturally hydrophilic mineral and thus it could be assumed that, when not treated with a collector, all the mass pull of these tests was due to entrainment [9].

The second subset was formed by the PRA Flota experiments. In these tests, the effects of particle size (coarse, medium, fine) and different frothers/combinations of frothers were supposed to be studied to find the optimal parameters for the separation of chalcopyrite from the Pyhäsalmi ore sample. This set of experiments was originally supposed to contain a total of 30 flotation tests but, due to the fact that our mill could not provide us with the finest fraction that we wanted to study, the plan was abandoned and a new one was formulated (the Pre-Thesis Flotation experiments). These 30 PRA tests were also supposed to be carried out in a randomized order and this is the reason behind the numbering of each experiment.

The third subset was formed by the Pre-Thesis Flotation experiments. Unlike in the PRA experiments, in the Pre-Thesis experiments the particle size (milling time) was no longer considered a variable, and instead we went for the finest obtainable feed in

all these tests. The milling times, however, varied for different feeds (Crushed / Freezedried ore), and due to the fact that some optimization needed to be done in the beginning (crushed ore milling times at first 25min and settled to 30min, Freezedried at first 10min and settled to 5min). In these tests, combinations of various collector, depressant, and frother concentrations were studied to first optimize the chalcopyrite separation with the commercial NF240 frother. Once the optimal conditions were reached, these parameters were used to test the separation efficiency with HPMC 40-60. Based on this result, the collector, depressant, and frother concentrations were further optimized for HPMC.

4.3.2 Flotation Experiments

When formulating the experimental plan for this thesis, the results obtained from the preliminary experiments served as a guideline for the parameters that were decided to be utilized and studied. Throughout the experimental phase, the research remained a living entity, and the plan was often adjusted along the way, whenever the fresh results obtained opened up an interesting direction for further investigation. To distinguish these experiments from the preliminary work, they are headlined as "Flotation Experiments", and referred to in the text as Thesis Flotation / Thesis Flota or "TF" for short. Based on the studied feed materials, chemicals, and experimental procedures, these experiments can be divided into three subsets.

The first subset (overall subset 4) contained the short interval experiments (TFs 1-7, 11-13, 18-19) done with HPMC 40-60. Since the preliminary experiments indicated that with HPMC 40-60 virtually all of the separation takes place during the first 6

59

minutes, a decision was made to zoom-in on these kinetics to study the separation more thoroughly. In these experiments, the first five fractions had intervals of 30 seconds (hereby referred to as "short intervals". In addition, experiment 10 (with 1 minute "medium" intervals) can be counted as a part of this subset.

The second subset (overall subset 5) was formed by the repetitive/preparative NF240 experiments (TFs 8-9, and, 14-17), that were performed to check for the reproducibility of the experiments, and to study the effectiveness of milling to the newly changed feed material (PS Natural ore). These experiments included re-runs of the Pre-Thesis Flota 7 experimental setup, with different feeds (Freezedried / PS Natural ore), milling times, and pH regulators (NaOH / (Ca(OH)$_2$)).

Finally, the third subset (overall subset 6) consisted of TFs 20, and 30-37, in which in-mill conditioning (excluding TF20), and frother additions to the added water were introduced. In these tests, the lower molecular weight polymer frother HPMC 10K (utilized previously in the preliminary Pre-Thesis Flota 8) was also revisited. In between subsets 5 and 6, nine experiments were performed that were not part of this thesis, and this is the reason for the absence of experiments 21-29.

In the end, a total of 28 experiments were performed under this experimental plan.. The experiments, and their experimental setups, are presented in *Table 9*.

Table 9: The experimental plan for the Thesis Flotation experiments.

Name	Frother(s) / Concentration(s) [ppm]	Milling Time [min]	pH Control (Chemical Used)	Amount of SIBX [g/t] / ZnSO₄ [g/t]	Feed Material	Remarks
Thesis Flota 1	HPMC 40-60 / 40ppm	5min	pH 12 (NaOH)	20 g/t + 500 g/t	PS Ore Freezedried	Short Intervals
Thesis Flota 2	HPMC 40-60 / 40ppm	5min	pH 12.4 (Ca(OH)₂)	20 g/t + 500 g/t	PS Ore Freezedried	Short Intervals
Thesis Flota 3	HPMC 40-60 / 30ppm	5min	pH 12.4 (Ca(OH)₂)	20 g/t + 500 g/t	PS Ore Freezedried	Short Intervals
Thesis Flota 4	HPMC 40-60 / 30ppm	5min	pH 12.4 (Ca(OH)₂)	30 g/t + 500 g/t	PS Ore Freezedried	Short Intervals
Thesis Flota 5	HPMC 40-60 / 24ppm	5min	pH 12.4 (Ca(OH)₂)	20 g/t + 500 g/t	PS Ore Freezedried	Short Intervals
Thesis Flota 6	HPMC 40-60 / 30ppm	5min	pH 12.4 (Ca(OH)₂)	10 g/t + 500 g/t	PS Ore Freezedried	Short Intervals + Broken pipette suspected
Thesis Flota 7	HPMC 40-60 / 30ppm	5min	pH 12.4 (Ca(OH)₂)	10 g/t + 500 g/t	PS Ore Freezedried	Short Intervals
Thesis Flota 8	NF240 / 24ppm	5min	pH 12 (NaOH)	30 g/t + 500 g/t	PS Ore Freezedried	
Thesis Flota 9	NF240 / 24ppm	5min	pH 12.4 (Ca(OH)₂)	30 g/t + 500 g/t	PS Ore Freezedried	
Thesis Flota 10	HPMC 40-60 / 30ppm	30min	pH 12.4 (Ca(OH)₂)	20 g/t + 500 g/t	PS Ore Natural	Intervals: 0-1min,

						1-2min, 2-3min
Thesis Flota 11	HPMC 40-60 / 30ppm	30min	pH 12.4 (Ca(OH)₂)	70 g/t + 500 g/t	PS Ore Natural	Short Intervals
Thesis Flota 12	HPMC 40-60 / 40ppm	30min	pH 12.4 (Ca(OH)₂)	70 g/t + 500 g/t	PS Ore Natural	Short Intervals
Thesis Flota 13	HPMC 40-60 / 30ppm	30min	pH 12.4 (Ca(OH)₂)	100 g/t + 500 g/t	PS Ore Natural	Short Intervals
Thesis Flota 14	NF240 / 24ppm	30min	pH 12 (NaOH)	30 g/t + 500 g/t	PS Ore Natural	
Thesis Flota 15	NF240 / 24ppm	35min	pH 12 (NaOH)	30 g/t + 500 g/t	PS Ore Natural	
Thesis Flota 16	NF240 / 24ppm	45min	pH 12 (NaOH)	30 g/t + 500 g/t	PS Ore Natural	
Thesis Flota 17	NF240 / 24ppm	45min	pH 12.4 (Ca(OH)₂)	30 g/t + 500 g/t	PS Ore Natural	
Thesis Flota 18	HPMC 40-60 / 30ppm	45min	pH 12.4 (Ca(OH)₂)	100 g/t + 500 g/t	PS Ore Natural	Short Intervals
Thesis Flota 19	HPMC 40-60 / 30ppm	45min	pH 12.4 (Ca(OH)₂)	100 g/t + 500 g/t	PS Ore Natural	Short Intervals
Thesis Flota 20	NF240 / 20ppm	45min	pH 12.4 (Ca(OH)₂)	30 g/t + 500 g/t	PS Ore Natural	Frother also in the added water
Thesis Flota 30	HPMC 40-60 / 30ppm	45min	pH 12.4 (Ca(OH)₂)	30 g/t + 500 g/t	PS Ore Natural	In-mill conditioning + Frother also in the added water

Thesis Flota 31	NF240 / 30ppm	45min	pH 12.4 $(Ca(OH)_2)$	30 g/t + 500 g/t	PS Ore Natural	In-mill conditioning + Frother also in the added water
Thesis Flota 32	NF240 + HPMC 40-60 / 16ppm+16ppm	45min	pH 12.4 $(Ca(OH)_2)$	30 g/t + 500 g/t	PS Ore Natural	In-mill conditioning + Frothers also in the added water
Thesis Flota 33	NF240 + HPMC 40-60 / 16ppm+16ppm	45min	pH 12.4 $(Ca(OH)_2)$	30 g/t + 500 g/t	PS Ore Natural	In-mill conditioning +30 mg Na_2SO_3 + Frother also in the added water
Thesis Flota 34	HPMC 40-60 / 50ppm	45min	pH 12.4 $(Ca(OH)_2)$	30 g/t + 500 g/t	PS Ore Natural	In-mill conditioning + Frother also in the added water
Thesis Flota 35	NF240 + HPMC 10K / 16ppm+16ppm	45min	pH 12.4 $(Ca(OH)_2)$	30 g/t + 500 g/t	PS Ore Natural	In-mill conditioning + Frothers also in the added water

Thesis Flota 36	NF240 + HPMC 10K / 10ppm+20ppm	45min	pH 12.4 (Ca(OH)$_2$)	30 g/t + 500 g/t	PS Ore Natural	In-mill conditioning + Frothers also in the added water
Thesis Flota 37	NF240 + HPMC 10K / 20ppm+10ppm	45min	pH 12.4 (Ca(OH)$_2$)	30 g/t + 500 g/t	PS Ore Natural	In-mill conditioning + Frothers also in the added water

4.4   Execution of the Experiments

4.4.1   Preliminary Experiments

In the beginning of the experiments, an amount of ore/quartz was weighed to match 600g of dry ore content. Additionally, pure water was weighed so that the water content of the ore and the pure water combined matched 600g. Depending on the experiment, the pH of the water was adjusted by adding an appropriate amount of 1M NaOH, or left as is. The pH level was monitored using an indicator paper. The ore-water suspension was subsequently ground in a ball mill with 50:50 dry-wet ratio for a specific amount of time, depending on the ore being used. After grinding, the mill was washed with additional 600g of purified/pH adjusted water, to achieve the aspired 33:67 dry-wet ratio for the flotation experiments.

After milling, the ore-water suspension was stirred for 5 minutes with 1300 rpm. Thereafter, the stirring speed was lowered to 900 rpm, and the chemicals were added to the suspension. The order of the chemical additions was depressant first, collector second, and frother(s) last. After each chemical addition, the system was given 3 minutes of time to mix, and for the surface-active reagents to adsorb (i.e. conditioning period). The experiments with mixed NF240 & HPMC made an exception, as the NF240 was added first and the HPMC immediately afterwards.

After the chemicals had been added, the stirring speed was increased back to 1300 rpm, and the air flow was set to 4L/min, which marked the beginning of the flotation process. As froth started to rise on the top of the suspension surface, it was scraped off on to a plate/container with a spatula. To monitor the kinetics of the process, the plate/container was replaced with a new one at 3, 6, 10, 14, and 20 minutes. When the plates were changed, pure water (or pH adjusted) was also added, to match the amount water that had left the system during the scrapings, and to keep the suspension surface at a roughly constant height in the flotation cell. The added amounts of water were also measured. For some of the Thesis Flota experiments, frother(s) was/were also supplemented to the added water, to keep the frother concentration constant throughout the experiment. These tests can be identified from *Table 9* by the "(also in added water)" note in the "Frother(s)" column.

The experiment was called off at 30 minutes, or at a time the froth production had ended. The amounts of scrapings for different fractions are located in *Table 10*.

Table 10: Flotation experiment regular fractions and number of scrapings.

Fraction	Number of Scrapings
0-3min	10 times every 30 seconds
3-6min	10 times every 30 seconds
6-10min	10 times every 30 seconds
10-14min	15 times every 1 minute
14-20min	15 times every 1 minute
20-30min	20 times every 2 minutes

Froth fractions of smaller volume were collected straight on to a plate, whereas larger fractions were first collected on larger containers, and thereafter filtered to fit on the plates. Also, the tailings were filtered and put on a plate as well. The plates were then placed in a hot air oven for the samples to dry. To avoid any large-scale oxidation of the ore, the temperature was kept at 50°C. The samples were left to dry for approximately 40 hours.

4.4.2 Flotation Experiments

The Thesis Flotation experiments were, in general, performed in a similar manner to the preliminary experiments. However, for some experiments, the procedure was slightly altered, and these experiments are discussed in this chapter.

For TFs 1-7, 11-13, and 18-19, a closer look on the kinetics of the first 3 minutes of flotation was made, and the corresponding fractions with shorter time intervals (and amounts of scrapings) are located in *Table 11*. The tests, in which these special

intervals were used, can also be identified from *Table 9* by the "Short Intervals" note in the remarks column. Also, for TF10, special intervals of 0-1min, 1-2min, and 2-3min were used (20 scrapings each – intervals noted in the remarks column of *Table 9*).

Table 11: The fractions and amounts of scrapings in the "short interval" tests.

Fraction	Number of Scrapings
0-30s	10 times
30-60s	10 times
60-90s	10 times
90-120s	10 times
120-150s	10 times
3-6min	10 times every 30 seconds

For TFs 20, and 30-37, frother(s) was/were added also in the water that was poured in the system in between fractions to keep the suspension surface at the same level. Doing so ensured, that the frother concentration of the pulp remained constant during the whole experiment.

Finally, in TFs 30-37, in-mill conditioning was used. In these experiments, depressants and collectors were added during the grinding period in the following manner:

1) Milling time = 0min: No chemicals added

2) Milling time = 15min: $ZnSO_4$ added

3) Milling time = 30min: SIBX added

After 45 minutes of grinding, the pulp was stirred for 5 minutes (at 1300 rpm), after which the stirring speed was lowered (900 rpm), and the forther(s) added. After the frother addition(s), the mix was allowed to be conditioned for a final 3 minutes, time after which the flotation experiment proceeded normally (rpm back to 1300, air in). Additionally, in Thesis Flotation experiment 33, sodium sulfite (Na_2SO_3) was studied for its suggested pyrite depressing ability [73] [74]. In this test, 30mg of dry powdery Na_2SO_3 was added in the mill at milling time t = 0min, and from there on, the experiment proceeded as other in-mill conditioned ones did.

4.4.3 Characterization

Once the samples had dried, they were moved from the plates into small plastic bags and weighed. For chemical analysis, a handheld XRF gun was used. The measurement mode was set to "Mining HighS" (a mode for sulfide-containing ores), and the time for a single measurement to 30 seconds. In addition, an average mode was used, so that five measurements were done on each sample fraction, and the averages of the results were calculated. In each measurement, the gun was pointed at a different part of the sample to avoid any biased results. The particle size analysis of the feed materials, done prior to the experiments, can also be regarded as a characterization procedure.

4.4.4 Calculations

Based on the mass pulls and the XRF results of the experiments, the separation efficiency, the cumulative recovery of the mineral, and the total grade in the froth were calculated for each test. These calculations were performed for the valuable copper containing chalcopyrite, and also for zinc and iron containing minerals to monitor the separation of these unwanted metals. The cumulative mineral recovery, the calculations were performed as indicated by *Eq. (6)*.

$$R_c = \sum_{t=0min}^{t=30min} \frac{i \cdot m}{m_{tot}} \tag{6}$$

Where,

R_c = Cumulative recovery of the particular mineral [%]

i = Amount of the particular mineral in a fraction (provided by XRF) [wt. %]

m = The mass of the corresponding fraction [g]

m_{tot} = The total mass of the particular mineral in the system [g]

The cumulative grade in froth (metal in the concentrate) was calculated as shown in *Eq. (7)*, after each fraction at time t=n (n=3min, 6min, 10min, 14min, 20min, 30min).

$$c = R_{c\_n} / m_{tot\_n} \tag{7}$$

Where,

c = Metal in the concentrate [%]

R_{c_n} = Cumulative recovery of the mineral (at time t=n) [g]

m_{tot_n} = Total mass pull of the experiment (at time t=n) [g]

For calculating the separation efficiency, *Eq. (8)* shown below was used [10].

$$SE = R_m - R_g = \frac{100\ C\ m\ (c-f)}{(m-f)\ f} \tag{8}$$

Where,

SE = Separation Efficiency [%]

R_m = Recovery of the valuable mineral [%]

R_g = Recovery of the gangue into the concentrate [%]

C = Fraction of total feed weight that reports to the concentrate [%]

f = Metal in the feed [%]

c = Metal in the concentrate [%]

m = Metal content in the mineral [%]

5 Results

5.1 Particle Size Analysis of the Feed Materials

The feed-specific milling time intervals, status of sonication for the samples where ultrasound was used (pre-/post-ultra), and total milling times, along with the dx10, dx50, and dx90 values are represented in *Table 12*.

Table 12: Results of the milling tests for each feed material.

NILSIÄ QUARTZ	dx10 [µm]	dx50 [µm]	dx90 [µm]
As is	150	334	628
As is	138	306	588
As is	136	307	585
2.5min	131	296	525
5min	113	271	475
7.5min	85.3	232	415
10min	59.6	184	340
15min	42.9	158	297
PS FREEZEDRIED ORE	dx10 [µm]	dx50 [µm]	dx90 [µm]
As is	7.85	53.5	173
As is	6.34	53.2	179
1min	12.6	91.3	220
2min	16.8	93.8	204

3min	14.7	89.2	207
5min Pre-Ultra	6.55	48.3	126
5min Post-Ultra	5.55	43.3	115
10min	5.53	39.4	107
PS ORE CRUSHED	**dx10 [μm]**	**dx50 [μm]**	**dx90 [μm]**
10min	50.9	210	424
15min	27.2	125	278
20min	13.5	90.7	209
25min	14.3	80.4	180
27.5min	11.2	70.5	169
30min	9.53	58.1	145
PS ORE SIEVED	**dx10 [μm]**	**dx50 [μm]**	**dx90 [μm]**
2.5min	56.6	480	1740
5min	34.1	171	434
7.5min	26.7	171	351
10min	24.9	165	347
12.5min	24.7	136	289
15min	15.1	89.5	203
17.5min	14.1	85.5	191
20min	13.8	84.4	188
22.5min	9.25	65.4	152
25min	8.71	59.8	142
27.5min	6.43	47.6	123
30min	7.07	49	119

PS NATURAL ORE	dx10 [μm]	dx50 [μm]	dx90 [μm]
45min	7.47	40.5	115

5.2 Masses of the Froth Fractions and Added Water

5.2.1 Preliminary Experiments

The masses of each froth fraction for the Quartz experiments are shown in *Table 13*. In this table, the dry mass of each froth fraction is presented in grams, and their combined weight (the total mass pull of the experiment) is presented in the "Total 0-30min" column. Furthermore, the weights of the tailings (in grams) are marked as well.

Table 13: The masses of the froth fractions for the Quartz experiments.

	0-3min	3-6min	6-10min	10-14min	14-20min	20-30min	Total 0-30min	Tailings
Quartz Flota 1	8.1	6.7	6.6	6.9	5.4	5.6	39.3	554
Quartz Flota 2	36.2	1.4	1.0	0	0	0	38.6	559.8
Quartz Flota 3	22.0	4.1	4.3	1.9	2.7	2.4	37.4	557.2

Also, *Fig. 31* shows the cumulative recoveries of the quartz experiments.
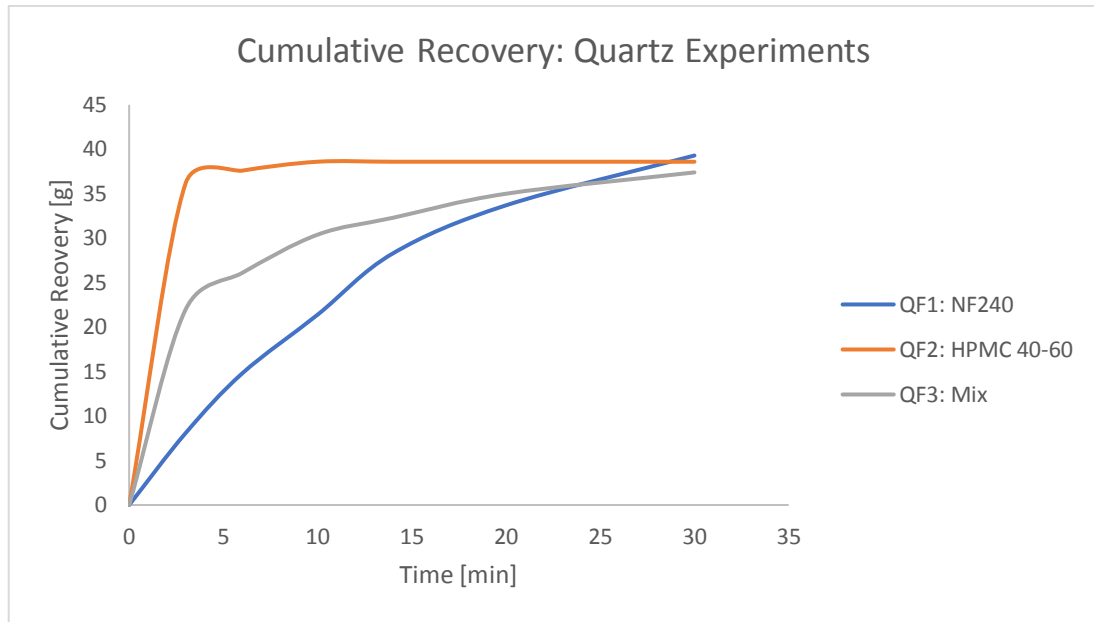
Figure 31: The cumulative recoveries of the quartz flotation (QF) experiments.

In addition, *Table 14* presents the values of water additions (in grams) in the quartz experiments. During the experiments, the water additions were always performed immediately after the fractions were completed. Therefore, for example in "Quartz Flota 1", the water addition of 293.5g has been done at time t=3min. Furthermore, the combined water consumption of the experiment is presented in the "Total 0-30" column.

Table 14: The masses of the added water for each fractions in the quartz experiments.

	0-3min	3-6min	6-10min	10-14min	14-20min	20-30min	Total 0-30min
Quartz Flota 1	293.5	208.5	248.3	216.4	184.9	209.8	1361.4
Quartz Flota 2	498.0	104.8	0	0	0	0	602.8
Quartz Flota 3	403.5	166.6	186.4	94.5	105.4	0	956.4

The masses of each froth fraction for the PRA experiments are shown in *Table 15*. In this table, the dry mass of each froth fraction is presented in grams, and their combined weight (the total mass pull of the experiment) is presented in the "Total 0-30min" column. Furthermore, the weights of the tailings (in grams) are marked as well. The water additions for these tests can be located in Appendix II.

Table 15: The masses of the froth fractions for the PRA experiments.

	0-3min	3-6min	6-10min	10-14min	14-20min	20-30min	Tailings	Total 0-30min
PRA Flota 1	103	66.9	63.2	37.9	49.5	43	237.5	363.5
PRA Flota 4	10	9.9	8.2	4.5	4.9	4.7	557.4	42.2
PRA Flota 13	130.7	106.0	94.7	52.5	42.3	26.4	121.2	452.6
PRA Flota 22	1.6	0	0	0	0	0	595.5	1.6
PRA Flota 23	4.3	0	0	0	0	0	602.4	4.3
PRA Flota 26	153.9	90.1	51	18.2	18.9	13.2	249.3	345.3
PRA Flota 28	9.7	10.4	8.4	3.4	5.8	7.1	552.3	44.8

Additionally, the masses of each froth fraction for the Pre-Thesis experiments are shown in *Table 16*. In this table, the dry mass of each froth fraction is presented in grams, and their combined weight (the total mass pull of the experiment) is presented in the "Total 0-30min" column. Furthermore, the weights of the tailings (in grams) are marked as well. The water additions for these tests can be located in Appendix II.

Table 16: The masses of the froth fractions for the Pre-Thesis experiments.

	0-3min	3-6min	6-10min	10-14min	14-20min	20-30min	Tailings	Total 0-30min
Pre-Thesis Flota 1	77.2	69.1	50.6	17.8	18.2	18.0	339.7	250.9
Pre-Thesis Flota 2	47.9	65.5	51.0	21.2	20.8	17.0	369.5	223.4
Pre-Thesis Flota 3	33.4	44.5	38.8	15.7	14.6	14.5	423.8	161.5
Pre-Thesis Flota 4	14.4	16.3	19.2	10.9	12.5	11.4	507.0	84.7
Pre-Thesis Flota 5	12.0	11.9	16.1	10.4	12.7	13.1	519.3	76.2
Pre-Thesis Flota 6	8.1	20.0	20.9	10.0	9.6	7.9	522.0	76.5
Pre-Thesis Flota 7	15.8	16.8	17.9	9.5	9.3	8.6	517.3	77.9
Pre-Thesis Flota 8	4.2	0		0	0	0	591.0	4.2
Pre-Thesis Flota 9	0	0	0	0	0	0	600	0
Pre-Thesis Flota 10	0	0	0	0	0	0	600	0
Pre-Thesis Flota 11	283.2	0	0	0	0	0	274.2	283.2
Pre-Thesis Flota 12	229.6	19.2	6.3	0	0	0	329.6	255.1
Pre-Thesis Flota 13	173.1	3.9	0	0	0	0	395.1	177.0
Pre-Thesis Flota 14	165	4.3	0	0	0	0	419.4	169.3
Pre-Thesis Flota 15	148.4	2.5	0	0	0	0	438.0	150.9

Furthermore, *Fig. 32* shows the cumulative recoveries of Pre-Thesis 7 (NF240) and Pre-Thesis 15 (HPMC 40-60). These experiments were chosen to be compared to illustrate the kinetic difference in the separation of the HPMC 40-60 and NF240. The experimental parameters of these two tests are not completely similar, but their comparison is still justified, as this trend (faster kinetics of HPMC) is clearly visible regarding all the experiments, in which the HPMC concentration has been sufficient enough for froth formation.
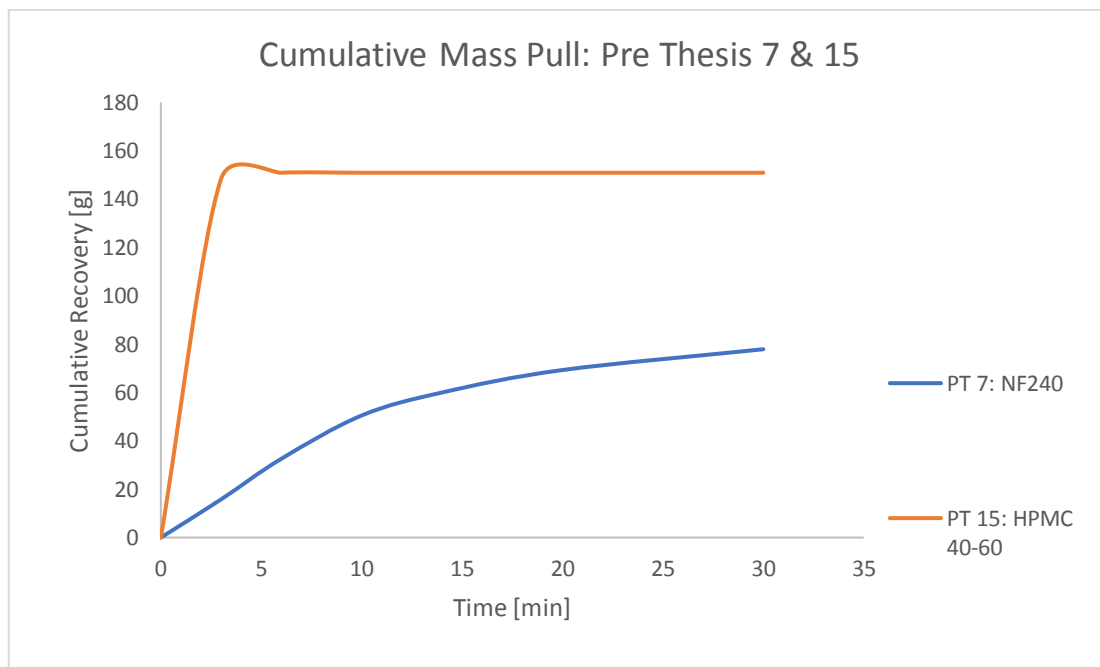
Figure 32: The cumulative recoveries of Pre-thesis 7 and Pre-Thesis 15.

5.2.2 Flotation Experiments

The masses of each froth fraction for the Thesis Flotation experiments are shown in *Table 17*. In this table, the dry mass of each froth fraction is presented in grams, and their combined weight (the total mass pull of the experiment) is presented in the "Total 0-30min" column (in grams as well). Furthermore, the masses of the tailings (in grams)

are marked as well. The experiments in which short time intervals were utilized are marked with red in this table (corresponding to the short interval fraction times marked with red). The water additions for these experiments can be located in Appendix II.

Table 17: The masses of the froth fractions for the Thesis Flotation experiments.

	0-3min / 0-30s	3-6min / 30-60s	6-10min / 60-90s	10-14min / 90-120s	14-20min / 120-150s	20-30min / 3-6min	Tailings	Total 0-30min / 0-6min
Thesis Flota 1	39.6	32.1	19.7	13.6	7.2	4.4	431.7	116.6
Thesis Flota 2	24.5	25.9	25.9	30.3	13.3	3.2	460.1	123.1
Thesis Flota 3	16.5	22.0	22.7	8.4	2.7	1.0	497.7	73.3
Thesis Flota 4	24.7	45.9	46.9	18.6	15.2	8.0	420.8	159.3
Thesis Flota 5	10.2	9.4	6.3	2.2	3.0	0	549.2	31.1
Thesis Flota 6	10.4	12.1	5.1	3.1	3.0	7.0	551.5	40.7
Thesis Flota 7	12.9	18.7	12.8	4.8	5.3	12.8	521.1	67.3
Thesis Flota 8	184.1	14	8.4	4.8	6.5	6.8	372.0	224.6
Thesis Flota 9	0	0	0	0	0	0	0	0
Thesis Flota 10	3.8	2.2	2.5				595.6	8.5
Thesis Flota 11	9.3	15.3	7.5	5.7	14.6	31.5	513.6	83.9
Thesis Flota 12	28.9	44.6	33.5	18.7	26.3	68.8	349.5	220.8
Thesis Flota 13	21.7	48.5	44.1	16.2	16.4	24.7	432.8	171.6
Thesis Flota 14	16.9	10.6	14.8	8.9	11.2	11.7	523.5	74.1
Thesis Flota 15	21.7	10.8	23	11.8	11.0	11.1	516.8	89.4
Thesis Flota 16	17.3	17.6	22.9	12.9	12.0	16.8	499.7	99.5
Thesis Flota 17	20.5	13.9	17.5	13.9	14.6	18.5	498.6	98.9

Thesis Flota 18	10.0	4.9	7.2	11.2	26.7	34.3	502.2	94.3
Thesis Flota 19	11.6	16.0	24.8	27.3	34.3	21.4	460.7	135.4
Thesis Flota 20	21.3	25.5	26.8	13.5	16.9	14.5	490.3	118.5
Thesis Flota 30	20.9	0	0	0	0	0	584.4	20.9
Thesis Flota 31	23.1	16.0	17.4	10.3	14.7	12.6	500.5	94.1
Thesis Flota 32	41.9	27.8	32.0	23.2	36.8	29.9	407.2	191.6
Thesis Flota 33	45.3	31.5	47.7	40.2	37.0	26.5	366.4	228.2
Thesis Flota 34	95.9	61.6	87.3	0	0	0	361.4	244.8
Thesis Flota 35	26.1	21.4	27.5	19.4	22.7	21.1	464.2	138.2
Thesis Flota 36	25.3	14.8	23.7	22.0	22.2	24.2	465.0	132.2
Thesis Flota 37	25.2	20.7	26.3	14.1	17.1	18.2	482.4	121.6

5.3 Grades, Recoveries, and Separation Efficiencies

5.3.1 Preliminary Experiments: Copper

Table 18 shows the values of the head grades [calculated - %], total grades in froth [%], cumulative recoveries of copper [%], and the maximum separation efficiencies (SE) [%] for copper in the preliminary experiments. The best performance (separation efficiency-wise - Pre-Thesis Flota 7) is highlighted. The experiments in which no notable froth formation happened (Pre-Thesis Flota 9 & 10) are left blank. The total grade in froth has been calculated based on the grades and masses of the individual fractions.

Table 18: The experiment-specific values for head grade, total grade in froth, cumulative recovery, and separation efficiency for copper.

	Head Grade (calculated)	Total Grade (in Froth)	Cumulative Recovery 0-30min	Max. SE
PRA Flota 1	1.00 %	1.43 %	86.68 %	26.98 %
PRA Flota 4	0.90 %	4.32 %	33.80 %	27.48 %
PRA Flota 13	1.13 %	1.36 %	94.94 %	18.61 %
PRA Flota 22	0.94 %	3.27 %	0.94 %	0.69 %
PRA Flota 23	0.91 %	4.14 %	3.22 %	2.58 %
PRA Flota 26	1.00 %	1.63 %	94.62 %	38.57 %
PRA Flota 28	0.96 %	4.06 %	31.65 %	24.84 %
Pre-Thesis Flota 1	1.05 %	1.82 %	73.85 %	32.35 %
Pre-Thesis Flota 2	0.99 %	1.87 %	71.42 %	34.80 %
Pre-Thesis Flota 3	0.98 %	2.08 %	58.54 %	31.85 %
Pre-Thesis Flota 4	0.87 %	3.43 %	56.45 %	43.23 %
Pre-Thesis Flota 5	0.93 %	3.49 %	47.91 %	36.09 %
Pre-Thesis Flota 6	0.65 %	3.39 %	66.69 %	54.94 %
Pre-Thesis Flota 7	**0.62 %**	**4.12 %**	**86.42 %**	**74.67 %**
Pre-Thesis Flota 8	0.72 %	0.93 %	0.91 %	0.21 %
Pre-Thesis Flota 9				
Pre-Thesis Flota 10				
Pre-Thesis Flota 11	1.48 %	0.57 %	19.46 %	-32.75 %
Pre-Thesis Flota 12	1.52 %	0.54 %	15.51 %	-28.38 %
Pre-Thesis Flota 13	0.91 %	1.55 %	52.57 %	22.21 %
Pre-Thesis Flota 14	0.88 %	1.46 %	48.06 %	19.80 %
Pre-Thesis Flota 15	0.94 %	1.67 %	45.65 %	20.58 %

5.3.2 Preliminary Experiments: Zinc

Table 19 shows the values of the head grades [calculated - %], total grades in froth [%], cumulative recoveries of zinc [%], and the maximum separation efficiencies [%] for zinc in the preliminary experiments. The experiments in which no notable froth formation happened (Pre-Thesis Flota 9 & 10) are left blank. The total grade in froth has been calculated based on the grades and masses of the individual fractions.

Table 19: The experiment-specific values for head grade, total grade in froth, cumulative recovery, and separation efficiency for zinc.

	Head Grade (calculated)	Total Grade (in froth)	Cumulative Recovery 0-30min	Max. SE
PRA Flota 1	1.82 %	1.58 %	52.27 %	-8.44 %
PRA Flota 4	1.75 %	5.51 %	22.15 %	15.51 %
PRA Flota 13	1.80 %	1.47 %	64.68 %	-14.59 %
PRA Flota 22	1.78 %	2.58 %	0.39 %	0.12 %
PRA Flota 23	1.75 %	2.87 %	1.16 %	0.46 %
PRA Flota 26	1.76 %	1.64 %	53.98 %	-4.20 %
PRA Flota 28	1.76 %	5.11 %	21.75 %	14.63 %
Pre-Thesis Flota 1	1.76 %	2.60 %	62.62 %	20.68 %
Pre-Thesis Flota 2	1.77 %	2.66 %	56.72 %	19.56 %
Pre-Thesis Flota 3	1.79 %	3.03 %	46.82 %	19.76 %
Pre-Thesis Flota 4	1.61 %	4.36 %	38.66 %	24.94 %
Pre-Thesis Flota 5	1.72 %	4.19 %	31.22 %	18.91 %
Pre-Thesis Flota 6	1.33 %	0.90 %	8.68 %	-0.11 %
Pre-Thesis Flota 7	1.22 %	1.18 %	12.69 %	-0.41 %

Pre-Thesis Flota 8	1.29 %	1.30 %	0.71 %	0.01 %
Pre-Thesis Flota 9				
Pre-Thesis Flota 10				
Pre-Thesis Flota 11	1.06 %	0.47 %	22.56 %	-28.70 %
Pre-Thesis Flota 12	1.18 %	0.42 %	15.46 %	-27.51 %
Pre-Thesis Flota 13	1.05 %	1.97 %	57.88 %	27.37 %
Pre-Thesis Flota 14	1.01 %	1.87 %	53.37 %	24.99 %
Pre-Thesis Flota 15	1.07 %	2.19 %	52.59 %	27.40 %

5.3.3 Preliminary Experiments: Iron

Table 20 shows the values of the head grade [calculated - %], total grades in froth [%], cumulative recoveries of iron [%], and separation efficiencies [%] for iron. The experiments in which no notable froth formation happened (Pre-Thesis Flota 9 & 10) are left blank. The total grade in froth has been calculated based on the grades and masses of the individual fractions.

Table 20: The experiment-specific values for head grade, total grade in froth, cumulative recovery, and separation efficiency for iron.

	Head Grade (calculated)	Total Grade (in froth)	Cumulative Revovery 0-30min	Max. SE
PRA Flota 1	30.19 %	31.99 %	64.09 %	10.22 %
PRA Flota 4	29.93 %	27.80 %	6.54 %	0.00 %
PRA Flota 13	30.85 %	32.87 %	84.06 %	15.94 %
PRA Flota 22	30.72 %	26.84 %	0.23 %	-0.10 %
PRA Flota 23	32.43 %	30.55 %	0.67 %	-0.13 %
PRA Flota 26	31.59 %	31.96 %	58.75 %	2.38 %

PRA Flota 28	30.71 %	29.13 %	7.12 %	-0.01 %
Pre-Thesis Flota 1	31.73 %	32.52 %	43.54 %	3.50 %
Pre-Thesis Flota 2	31.95 %	32.46 %	38.28 %	2.43 %
Pre-Thesis Flota 3	31.96 %	32.14 %	27.75 %	0.85 %
Pre-Thesis Flota 4	29.89 %	30.40 %	14.56 %	0.68 %
Pre-Thesis Flota 5	31.71 %	29.60 %	11.95 %	-0.56 %
Pre-Thesis Flota 6	31.18 %	31.94 %	13.09 %	1.09 %
Pre-Thesis Flota 7	31.51 %	31.12 %	12.93 %	0.15 %
Pre-Thesis Flota 8	31.45 %	31.24 %	0.70 %	-0.01 %
Pre-Thesis Flota 9				
Pre-Thesis Flota 10				
Pre-Thesis Flota 11	30.29 %	32.54 %	54.57 %	10.73 %
Pre-Thesis Flota 12	30.62 %	32.26 %	45.96 %	6.86 %
Pre-Thesis Flota 13	29.49 %	29.68 %	31.14 %	0.54 %
Pre-Thesis Flota 14	30.02 %	27.44 %	26.28 %	-6.93 %
Pre-Thesis Flota 15	30.07 %	28.47 %	24.26 %	-3.81 %

5.3.4 Flotation Experiments: Copper

Table 21 shows the values of the head grades [calculated - %], total grades in froth [%], cumulative recoveries of copper [%], and the maximum separation efficiencies [%] for copper. The best performances (TFs 35, 36, and 37) are highlighted. TF10, in which no notable froth formation happened, is left blank. The total grade in froth has been calculated based on the grades and masses of the individual fractions. For these experiments, the individual fraction grades can be found from Appendix III.

Table 21: The experiment-specific values for head grade, total grade in froth, cumulative recovery, and separation efficiency for copper in the Thesis Flota experiments.

	Head Grade (calculated)	Total Grade (in froth)	Cumulative Recovery 0-30min	Max. SE
Thesis Flotation 1	0.97 %	0.40 %	8.73 %	-4.82 %
Thesis Flotation 2	0.89 %	2.47 %	58.57 %	38.45 %
Thesis Flotation 3	0.84 %	3.88 %	59.39 %	47.71 %
Thesis Flotation 4	0.97 %	2.12 %	59.70 %	33.17 %
Thesis Flotation 5	0.97 %	3.72 %	20.51 %	15.59 %
Thesis Flotation 6	1.06 %	2.67 %	17.36 %	10.82 %
Thesis Flotation 7	0.97 %	2.11 %	24.96 %	13.91 %
Thesis Flotation 8	0.86 %	0.81 %	35.22 %	-2.49 %
Thesis Flotation 9	0,89 %	4,46 %	66,99 %	55,01 %
Thesis Flotation 10				
Thesis Flotation 11	0.60 %	1.68 %	39.52 %	25.92 %
Thesis Flotation 12	0.51 %	1.08 %	80.95 %	42.87 %
Thesis Flotation 13	0.63 %	1.63 %	73.02 %	45.46 %
Thesis Flotation 14	0.86 %	4.47 %	64.76 %	53.68 %
Thesis Flotation 15	0.86 %	4.14 %	71.17 %	57.86 %
Thesis Flotation 16	**0.89 %**	**4.52 %**	**84.46 %**	**69.64** %
Thesis Flotation 17	0.88 %	4.13 %	77.89 %	62.97 %
Thesis Flotation 18	0.91 %	0.29 %	5.01 %	-0.14 %
Thesis Flotation 19	0.81 %	0.22 %	6.00 %	-1.74 %
Thesis Flotation 20	0.93 %	4.07 %	85.19 %	67.54 %
Thesis Flotation 30	0.76 %	0.29 %	1.32 %	-2.18 %
Thesis Flotation 31	0.89 %	4.18 %	74.37 %	60.09 %
Thesis Flotation 32	0.87 %	2.60 %	95.16 %	66.10 %

Thesis Flotation 33	0.89 %	2.20 %	94.95 %	59.81 %
Thesis Flotation 34	0.88 %	0.96 %	43.69 %	3.39 %
Thesis Flotation 35	**0.84 %**	**3.32 %**	**90.77 %**	**69.51 %**
Thesis Flotation 36	**0.89 %**	**3.61 %**	**89.57 %**	**69.22 %**
Thesis Flotation 37	**0.86 %**	**3.66 %**	**85.86 %**	**67.40 %**

5.3.5 Flotation Experiments: Zinc

Table 22 shows the values of the head grades [calculated - %], total grades in froth [%], cumulative recoveries of zinc [%], and the maximum separation efficiencies [%] for zinc. TF10, in which no notable froth formation happened, is left blank. The total grade in froth has been calculated based on the grades and masses of the individual fractions.

Table 22: The experiment-specific values for head grade, total grade in froth, cumulative recovery, and separation efficiency for zinc in the Thesis Flota experiments.

	Head Grade (calculated)	Total Grade (in froth)	Cumulative Recovery 0-30min	Max. SE
Thesis Flotation 1	1.23 %	0.78 %	13.58 %	-3.58 %
Thesis Flotation 2	0.98 %	3.53 %	75.59 %	55.29 %
Thesis Flotation 3	0.91 %	5.88 %	82.52 %	70.65 %
Thesis Flotation 4	1.10 %	3.13 %	78.38 %	51.77 %
Thesis Flotation 5	1.07 %	6.29 %	31.44 %	26.50 %
Thesis Flotation 6	1.15 %	4.73 %	28.17 %	21.67 %
Thesis Flotation 7	1.17 %	3.69 %	36.22 %	25.22 %

Thesis Flotation 8	0.49 %	0.59 %	46.01 %	8.43 %
Thesis Flotation 9	1,03 %	3,75 %	48,76 %	35,91 %
Thesis Flotation 10				
Thesis Flotation 11	1.34 %	0.19 %	2.02 %	-1.29 %
Thesis Flotation 12	1.09 %	0.19 %	6.81 %	-3.82 %
Thesis Flotation 13	1.14 %	0.24 %	6.05 %	-2.73 %
Thesis Flotation 14	1.24 %	1.31 %	13.12 %	0.74 %
Thesis Flotation 15	1.29 %	1.46 %	16.67 %	1.96 %
Thesis Flotation 16	1.12 %	1.72 %	25.47 %	9.01 %
Thesis Flotation 17	1.14 %	1.40 %	20.34 %	3.85 %
Thesis Flotation 18	1.29 %	0.21 %	2.57 %	-0.39 %
Thesis Flotation 19	1.15 %	0.10 %	1.96 %	-1.76 %
Thesis Flotation 20	1.29 %	1.43 %	21.57 %	2.15 %
Thesis Flotation 30	1.02 %	0.31 %	1.04 %	-2.45 %
Thesis Flotation 31	1.23 %	1.80 %	23.17 %	7.48 %
Thesis Flotation 32	1.28 %	1.67 %	41.59 %	9.78 %
Thesis Flotation 33	1.26 %	1.51 %	46.05 %	7.82 %
Thesis Flotation 34	1.25 %	0.65 %	21.15 %	-7.98 %
Thesis Flotation 35	1.17 %	2.06 %	40.22 %	17.59 %
Thesis Flotation 36	1.20 %	2.17 %	40.01 %	18.20 %
Thesis Flotation 37	1.21 %	2.17 %	36.29 %	16.45 %

5.3.6 Flotation Experiments: Iron

Table 23 shows the values of the head grades [calculated - %], total grades in froth [%], cumulative recoveries of iron [%], and the maximum separation efficiencies [%] for iron. TF10, in which no notable froth formation happened, is left blank. The total

grade in froth has been calculated based on the grades and masses of the individual fractions.

Table 23: The experiment-specific values for head grade, total grade in froth, cumulative recovery, and separation efficiency for copper in the Thesis Flota experiments.

	Head Grade (calculated)	Total Grade (in froth)	Cumulative Recovery 0-30min	Max. SE
Thesis Flotation 1	30.27 %	33.49 %	23.53 %	6.43 %
Thesis Flotation 2	30.74 %	29.07 %	19.96 %	-0.89 %
Thesis Flotation 3	30.50 %	26.88 %	11.31 %	-1.18 %
Thesis Flotation 4	30.74 %	30.45 %	27.20 %	-0.12 %
Thesis Flotation 5	30.70 %	27.71 %	4.84 %	-0.45 %
Thesis Flotation 6	31.44 %	29.22 %	6.39 %	-0.33 %
Thesis Flotation 7	30.89 %	30.75 %	11.39 %	0.16 %
Thesis Flotation 8	30.58 %	32.66 %	40.21 %	8.81 %
Thesis Flotation 9	30,45 %	29,04 %	12,77 %	0,13 %
Thesis Flotation 10				
Thesis Flotation 11	31.08 %	33.57 %	15.17 %	3.37 %
Thesis Flotation 12	29.07 %	34.45 %	45.87 %	18.97 %
Thesis Flotation 13	30.33 %	34.22 %	32.03 %	10.39 %
Thesis Flotation 14	30.35 %	28.99 %	11.84 %	-0.28 %
Thesis Flotation 15	31.20 %	29.45 %	13.92 %	-0.69 %
Thesis Flotation 16	29.05 %	29.73 %	16.99 %	1.03 %
Thesis Flotation 17	28.94 %	29.64 %	16.96 %	1.06 %
Thesis Flotation 18	31.07 %	33.97 %	17.29 %	4.42 %
Thesis Flotation 19	29.37 %	34.41 %	26.61 %	10.52 %

Thesis Flotation 20	30.70 %	30.92 %	19.61 %	0.69 %
Thesis Flotation 30	27.79 %	34.17 %	4.24 %	1.96 %
Thesis Flotation 31	30.55 %	29.79 %	15.43 %	0.30 %
Thesis Flotation 32	31.44 %	31.42 %	31.97 %	-0.08 %
Thesis Flotation 33	30.65 %	31.91 %	39.96 %	4.61 %
Thesis Flotation 34	31.60 %	32.32 %	41.31 %	2.86 %
Thesis Flotation 35	30.59 %	30.45 %	22.83 %	0.57 %
Thesis Flotation 36	30.37 %	31.31 %	22.83 %	1.98 %
Thesis Flotation 37	30.86 %	29.90 %	19.50 %	0.04 %

6 Discussions

6.1 Preliminary Experiments

6.1.1 Subset 1: Quartz Experiments and Level of Entrainment

The aim of the quartz experiments was to study the role that the unselective entrainment plays in the flotation-based copper separation – with both NF240 and HPMC 40-60. This could be done by comparing the mass pulls of the quartz experiments to the mass pulls of the ore experiments. Since quartz is a naturally hydrophilic mineral, all of its separation can be assumed to happen via entrainment (in the absence of activators/collectors).

When comparing the results of the quartz experiments (*Table 13*) with the tests done with the ores (*Table 15 & Table 16*), we can see both similarities and differences. With NF240 the most accurate comparison (between quartz and ore tests) can be done with

the "PRA Flota 4" since, in both cases, no collector or depressant has been used. The total mass pulls of these tests are virtually identical. This indicates that, with NF240, entrainment is definitely not a negligible method of separation. However, in the PRA 4 test, only 30ppm of frother has achieved this separation, whereas the quartz tests were done with 50ppm frother concentration. This means that true flotation still plays an important role in the separation as well. Also, it can be noted that quartz is not as heavy as the minerals in our ore, which makes it more easily entrained [68] (i.e. even with same frother concentrations the amount of material separated via entrainment is higher in the quartz experiments). The kinetics of these tests are also strikingly similar. The 0-3min fractions have the highest mass pull, and the subsequent fractions follow a slowly decreasing trend.

Between the quartz and HPMC 40-60 no complete comparison can be made since none of the HPMC 40-60 tests was performed with no collector and depressant present. However, *Table 13* shows that the mass pull due to entrainment is pretty much independent on the frother/mixture of frothers being used. As we know, based on the results shown in *Table 15* and *Table 16*, HPMC 40-60 tends to have a higher total mass pull compared to NF240. This means that, with HPMC 40-60, a smaller percentage of the mass pull can be assumed to happen via entrainment, and thus, HPMC 40-60 can be considered less vulnerable to entrainment than NF240. Also, it can be observed that the kinetics between the quartz and ore experiments done with HPMC 40-60 are very similar. In the case of the HPMC 40-60, virtually all of the separation happens during the first 3 minutes of the experiments (*Figs. 31 & 32*). At ca. 5 minutes, the froth production stops. This might indicate that, after those few minutes, as the HPMC 40-

60 is depleted of the system in the froth phase, its concentration in the pulp decreases below some critical value at which the bubble stabilizing behavior of the polymer disappears. This critical-concentration-hypothesis is further backed with the Pre-Thesis Flota 8, and 9 experiments, both of which did not have any froth production at all, at a 24ppm frother concentration.

The kinetics of the mixed frother test (*Table 13* and *Fig.31*) shows characteristics of both the single HPMC and NF240 tests, as there is a massive peak in the mass pull right at the beginning (HPMC 40-60-like behavior) but, rather than dying out altogether, the froth production continues until the very end of the experiment (NF240-like behavior). The physical appearance of the froth (during the first few minutes) was clearly distinguishable from either of the single frother tests. At the later stages of the flotation experiment, the froth resembled closely those produced using pure NF240. This further backs up the hypothesis of HPMC 40-60 losing its bubble stabilizing potential when its concentration decreases below a critical value.

6.1.2 Subset 2: The Copper Separation in the PRA Experiments

As already mentioned earlier, 30 flotation experiments were supposed to be conducted under the PRA-subset. In these tests, PSDs were supposed to be used as a test parameter, with three different milling times used to obtain a coarse, medium, and fine feed for the tests. However, as *Table 12* shows (the "Sieved feed" tests), the mill that was used hit a barrier at around 27.5min-30min mark and it couldn't grind the ore any finer. This was a shame, since the fine fraction would have been the most interesting one to study, as it would have had the best potential for the separation. Due to this, and

the fact that the achieved copper separation efficiencies were rather poor (as can be seen from *Table 18*), this experimental setup was abandoned and replaced with the newly-formulated Pre-Thesis experiments.

Although the desired results regarding the copper separation efficiency could not be obtained, the PRA subset still revealed some interesting information. During these experiments, a smaller molecular weight polymer frother HPMC 10K (PRA 22 and 23) was tested, and an observation was made that it did not produce basically any froth at all (*Table 15*). This indicated that either the polymer structure was inherently incapable of bubble stabilization, or that the critical bubble stabilizing concentration of HPMC 10K is bigger than the 30ppm that was used. Thus far, it was also known that the HPMC 40-60 did not produce froth at 24ppm. For upcoming experiments, it would be interesting to try to find the critical bubble stabilizing concentration for this frother as well.

6.1.3 Subset 3: Pre-Thesis Experiments & Optimization of the Chalcopyrite Separation

With the PRA-set of experiments, the copper separation proved challenging, as the highest achieved copper separation efficiency was only 38.57% (*Table 15*, PRA 26). The shortcomings with concentrating the copper, together with the problems regarding the use of the PSDs as a variable, made the original experimental plan challenging without a properly formulated exploratory work, and thus the aforementioned Pre-Thesis experiments (hereby referred to as Pre-TF) were carried out instead. With this setup, an acceptable separation efficiency (with NF240) of 74.67% was achieved

(*Table 18*, Pre-TF 7), and the parameters from this test were then utilized to test the separation efficiency with HPMC 40-60. Surprisingly, with these parameters the HPMC 40-60 produced no froth at all. This put the research back to square one, and a decision was made to increase the HPMC 40-60 concentration back to 50ppm, and later 40ppm. This brought back the froth production, but the promising values of copper separation efficiency were gone. From *Table 18*, we can see that none of the single-HPMC Pre-TF experiments provided any notable separation, with separation efficiencies ranging from -22 to the low 20s (best results with Pre-TF 13). However, it can already be seen, that lowering the collector concentration addition from 50 g/t to 30 g/t has improved the separation drastically (from -20 to 20). It is worth noting that, since these tests are done with the pre-conditioned freezedried ore, the total collector concentration is likely more.

6.1.4 Subsets 2 & 3: the Separation Efficiencies of Zinc and Iron

From *Table 19*, we can see that the separation efficiency of zinc is not only dependent on the concentration of the depressant but, also, the type/amount of frother, pH, and the concentration of the collector play an important role as well. With NF240, the optimal parameters for zinc depressing seem to be those of Pre-TF 6 and 7 (*Table 19*). With HPMC 40-60, the optimal parameters were not yet found. Some curious behavior can be observed between Pre-TF 12 and 13, in which a simple drop in the collector concentration from 50ppm to 30ppm has turned the zinc separation upside down. With the higher collector concentration, zinc has been enriched in the tailings, whereas the lower collector concentration enriches it to the froth. This behavior repeats even when the concentration of the original zinc depressant is increased to 500 g/t.

However, as *Table 20* shows, while the Zn separation has gone up in the Pre-TF 13, 14, and 15, the iron containing pyrite separation has followed a decreasing trend. Since pyrite is the most abundant constituent of the gangue (in the PS ore), these results indicated that a right course of action had been taken. Even if the Cu and Zn minerals could be effectively separated, a huge progress would be made. In the upcoming experiments, depression of the pyrite was taken as a main goal.

6.2   Towards the Flotation Experiments

The results obtained from these 28 preliminary experiments served as a ground work for the experimental plan of the Thesis Flotation experiments. Based on these results, it was decided to not use the particle size of the feed as a variable, but instead go for the finest obtainable PSD that the mill could provide, with all of the Thesis Flotation experiments. Also, the concentration of the sphalerite depressant ($ZnSO_4$) was decided to be kept constant at 500 g/t. Also, as the HPMC 40-60 was observed to have a huge peak in the mass pull during the first 3 minutes, for some of the upcoming experiments it was decided divide the first 3 minutes of the experiment into five fractions of 30 seconds each (the short-interval experiments). However, many of the results raised more questions than answers and, for example, the collector and frother concentrations were still left up for experimentation within the Thesis Flotation experimental plan.

6.3   Flotation Experiments

6.3.1   Subset 4: The Short Interval Experiments (TFs 1-7, 10-13, 18-19)

The first subset (subset 4 overall) of the TF experiments introduced the utilization of shorter time intervals in between fractions – namely 30 seconds for the first five fractions (0-150s), after which a normal 3-6min fraction proceeded. Since the kinetics of the HPMC 40-60-based separation were observed to be so fast, that basically all separation occurs within the first six minutes, it was seen interesting to zoom-in on these kinetics.

In the short interval experiments, the separation efficiency of copper varied from an unacceptable -4.82 % (*Table 21*: TF1) to a decent 47.71 % (*Table 21*: TF3). However, the separation was still quite poor compared to the benchmark 74.67 % achieved in Pre-TF 7 (*Table 18*). When looking at the results of these experiments, it can be stated that the HPMC 40-60-based separation seems to be somewhat vulnerable to excess frother concentration, and extremely vulnerable to excess amounts of collector, and the choice of the pH regulator.

As was noticed with the Pre-TF experiments, (*Table 18*) too high collector concentrations were detrimental for the copper separation. This behavior repeats with the TF experiments, as the worst results (i.e. negative separation efficiencies) were all obtained with high collector concentrations (70 g/t – 100 g/t on natural ore, TF 11-13, and TF 18-19). This behavior is suspicious, as with NF240, increasing the collector concentration does not result in a similar type of total loss of separation (*Table 21*: 70

g/t SIBX has achieved a decent copper separation efficiency of around 30 in tests Pre-TF 1-3).

The effect of the frother concentration seems to be peculiar as well. An interesting comparison can be done with TF experiments 2, 3, and 5. In these tests, the HPMC 40-60 concentration has been steadily lowered from 40ppm to first 30ppm, and then 24ppm, while keeping other parameters constant. In between, an extra test (TF4) was conducted with an increased collector concentration (freezedried ore: SIBX from 20 g/t to 30 g/t), while keeping the HPMC 40-60 concentration at 30ppm (same as TF3). The 40ppm and 30ppm HPMC 40-60 decrease seems to have virtually no effect on the cumulative recovery of copper, although the grade has increased noticeably with the lower frother concentration. Consequently, the separation efficiency of TF3 (30ppm HPMC 40-60) is much better than in TF2. However, when lowered to 24ppm (TF5), the HPMC 40-60 seems to have lost its froth stabilizing ability, resulting in such a low mass pull, that the separation efficiency is low as well . Furthermore, when lowering the HPMC concentration from 30ppm to 24ppm, the grade has stayed virtually the same. This result was still interesting, as it contradicted one of the previous findings that suggested that no froth formation at all happens with HPMC 40-60 concentration of 24ppm (Pre-TF 9). At this point, it was thought that 30ppm was the optimal concentration for the HPMC, and an effort was made to enrich this optimal froth with increasing the collector from 20 g/t to 30 g/t (TF4). However, this collector addition resulted again in the loss of grade, and the separation efficiency was unacceptable.

The most notable change in the HPMC 40-60-based copper separation occurred after the pH regulator was switched from NaOH to $Ca(OH)_2$. This was done for the first time in TF2, and the separation efficiency almost doubled compared to the best results obtained with NaOH (Pre-TF 11-13). This was expected, as $Ca(OH)_2$ has been known for its pyrite depressing ability within the context of flotation [75].

The copper grades of individual experiments can be found from Appendix III. These results show that, although the copper grade follows a decreasing trend (highest values in the first fractions), the change in the grade is not too drastic. These short interval experiments were first formulated to study the possibility that the system was so selective towards copper, that the majority of it would have been separated within seconds, not minutes of the start of the experiment. However, as Appendix III shows, the copper grades were quite similar within all the fractions between 0-150s.

An interesting aspect of TF experiments 1-7 is that the best copper separation is always associated with an even better zinc separation. This happens despite the fact, that a notable concentration (500 g/t) of $ZnSO_4$ is used to depress the zinc. This behavior is, however, not observed in TFs 11-13, in which higher collector concentrations are used. In TFs 11-13, Cu is slightly enriched and Zn stays depressed (separation efficiencies around 0 %). However, in TFs 11-13, the pyrite separation has increased, as its separation efficiencies are around 10 %, instead of 0 %, associated with the experiments with the best copper separation. In TFs 18-19, the chemical parameters are the same as TF13 (which had a relatively good copper separation), but the milling time is longer (increased to 45min that was thought to be optimal). Surprisingly, in TF

18-19 neither Zn nor Cu are separated, whereas pyrite is (*Tables 21*, *22*, and *23*). This could mean that either the extra collector somehow decreases the selectivity towards Zn, but increases it towards Fe, or this behavior is associated with solely the particle liberation. This could also be viewed as evidence for collector-like properties of HPMC 40-60, as the extra grinding time exposes a bigger mineral surface area for possible reaction with collectors (hypothetically HPMC 40-60), which could result in the increment of the pyrite separation on the expense of the Cu and Zn separation (although this difference could also be a result of the change in the feed batch between TFs 18-19 and TF 13). As stated earlier, pyrite depression is the single most important factor for a selective Cu flotation of our ore, as pyrite is the main constituent of our gangue. In an ideal case, the separation efficiency of Fe should be well below 0 %.

It seems like, within this chemical setup of collectors and depressants, the froth stabilizing capability of HPMC 40-60 only shows up at concentrations so high, that the selectivity of the process suffers (towards Cu). There is also the possibility, that the HPMC 40-60 has collector-like properties, in addition to its froth stabilizing properties. If this hypothesis was proven correct, the excess amount of HPMC 40-60 could be assumed to lower the Cu grade in a similar manner that is associated with the increment of the SIBX concentration. The performance of these experiments could be improved by depressing the pyrite and sphalerite more effectively. Cyanide-based depressants could be a possibility for pyrite [76], and for zinc, the $ZnSO_4$ concentration could perhaps be increased much higher than the 500 g/t that was used. In some studies, $ZnSO_4$ concentrations of up to 3500 g/t have been reported [77].

6.3.2 Subset 5: Pre-Thesis Flota 7 Re-Runs (TFs 8-9, 14-17)

The experiments in this subset introduced the same chemical parameters that were used earlier in Pre-Thesis Flota 7 (Pre-TF 7), which had the best copper separation efficiency of our preliminary experiments. The purpose of these tests was to check for the reproducibility of the experiments, as well as looking into the milling response of the new feed (PS Natural Ore first used in TFs 14-17). During this time, our particle size analysis machinery had suffered a temporary breakage, and the PSD of the new feed could not be verified with it.

In Thesis Flotation experiments 8 and 9 (TF8 and TF9), freezedried ore was used as a feed material. Consequently, when these experiments were performed with the Pre-TF 7 parameters, the mass pulls of the experiments were huge, compared to the original Pre-TF 7. This was due to the fact that the feeds were not compatible. Pre-TF 7 was performed with the unconditioned PS Crushed ore, whereas our freezedried ore was a fully conditioned one – meaning that collectors and activators had already been introduced into it at the Pyhäsalmi plant. The excess amount of chemicals introduced to it in the laboratory were most likely responsible for the increased mass pull, as the added collector adsorbed on the gangue mineral surfaces. This decreased the Cu grade, and drove the separation efficiency towards negative values.

However, as the feed was changed to the new PS Natural ore (unconditioned), the results got back on track. In TF 14-17, the results are already similar to Pre-TF 7. It can also be seen, that a grinding time of 45 minutes achieved the best results (almost identical to Pre-TF 7). This excess amount of grinding was needed, as the PS Natural

ore was sieved with a coarser sieve compared to the PS Crushed ore. Since the results were similar, a deduction was made that a grinding time of 45 minutes was optimal for the PS Natural ore. Later, as the PSA machine got fixed, this deduction was proven correct (*Table 12*). These experiments also showed, that the reproducibility of the experiments was on an acceptable level.

6.3.3 Subset 6: Constant Frother Concentration/ In-Mill Conditioning (TFs 20, 30-37)

In the final eight experiments of the thesis, constant frother levels, and in-mill conditioning for the chemical additions were introduced. In the previous experiments, the make-up water, that was added between fractions to keep the suspension surface level constant, was only pH controlled (if needed) and did not contain any frothers. This meant that, as the experiments went on, the frother concentration was constantly decreasing, as the frother molecules left the system in the froth phase. To provide a similar physico-chemical basis for the separation in the later stages of the experiments, frothers were added into the make-up water. The in-mill conditioning was a procedure that the Pyhäsalmi flotation plant was using, and it was adopted to the final experiments, to emulate the Pyhäsalmi process as precisely as possible. Furthermore, in TF33, sodium sulfite (Na_2SO_3) was tried as a potential pyrite depressant chemical.

In TF30, 30ppm of HPMC 40-60 was used, which again produced non-selective separation, with a low mass pull. TF20 and TF31 showed that NF240 worked as usual, resulting in a copper separation efficiency of around 60%. In TF32, an interesting result was obtained, as a mixture of HPMC 40-60 and NF240 was found to have a very

high copper recovery (95%), while maintaining a relatively good grade (2,6%). Somehow, it appears that while the HPMC (at low concentrations) cannot support froth stabilization on its own, it still contributes to it noticeably in the presence of NF240 (that works on lower concentration as well). In TF33, the test parameters were kept as in TF32, with the exception that sodium sulfite was added as a potential pyrite depressant. This did not work out, as pyrite was actually recovered more, perhaps following the suggestions in literature that too low or high concentrations of Na_2SO_3 can actually result in an increased pyrite recovery [73]. For TF34, it was once again tried to increase the HPMC 40-60 concentration to 50ppm, resulting in substantial froth formation, with the loss of grade. The final experiments (TF35-37) were done on mixtures of NF240 and the short chain cellulose frother HPMC 10K, that we had previously used in the PRA Flotations. Up until this stage, HPMC 10K was not given too much notice, as the PRA experiments 22 and 23 suggested its froth stabilizing ability, at least at the 24ppm concentration we applied, to be virtually inexistent. Most surprisingly, these experiments produced our best HPMC-related test results so far, with copper separation efficiencies of around 70 % that even rivaled the benchmark Pre-TF 7 copper separation efficiency of 74.67 %. Interestingly, the results of these final experiments (TFs 35-37) seem to be very similar with all of the studied frother ratios (50:50, 66:33, 33:66). These final and most promising results, together with the best reference result (Pre-TF 7) are gathered in *Table 24* below.

Table 24: The best copper separation efficiencies obtained in the experiments (both with NF240 and mixtures).

	Frother Concentration(s)	Concentrations of Other Chemicals	Separation Efficiency
Pre-Thesis Flota 7	24ppm NF240	500 g/t ZnSO4 30 g/t SIBX	74.67 %
Thesis Flota 35	16ppm NF240 + 16ppm HPMC 10K	500 g/t ZnSO4 30 g/t SIBX	69.51 %
Thesis Flota 36	10ppm NF240 + 20ppm HPMC 10K	500 g/t ZnSO4 30 g/t SIBX	69.22 %
Thesis Flota 37	20ppm NF240 + 10ppm HPMC 10K	500 g/t ZnSO4 30 g/t SIBX	67.40 %

These separation efficiencies, presented in *Table 24*, still do not come close to what the industry is able to achieve. This underlines the fact that flotation is a very process-specific method of separation, and the groundwork that needs to be done to understand the nature of a specific ore and its properties is immense. Furthermore, the specifications of certain process parameters is knowledge that is kept within the industry. However, it is important to realize, that even if the separation efficiencies are not yet at an industrially acceptable level, a reliable comparison between the commercial frother and the HPMCs can still be made. When this comparison is done, it can be seen that in these experiments the HPMCs did not seem to be able to produce copper separation on their own, whereas the mixtures were a lot more promising. In the TF experiments 35-37, the separation efficiency is already very close to the best results that were achieved with NF240. This opens the door for the possibility, that HPMC could be utilized to improve the environmental performance of flotation.

It looks like HPMC 40-60 forms very stable but unselective froths at concentrations succeeding certain threshold point (around 30ppm). From the quartz experiments, we have already deducted that HPMC 40-60 is not more vulnerable to entrainment than NF240. This low selectivity is due to something else than what the conventional flotation theory suggests. One hypothesis is that the adsorption of HPMC 40-60 results in lots of tail and loop structures (*Fig. 20*) which enables the hydrophilic OH groups of the hydroxypropyl parts to attach to certain non-hydrophobized minerals. Also, the OH groups located in the branches of the higher MS HPMCs could play a similar role as well. With HPMC 10K, the froth stabilizing ability looks to be virtually inexistent in low concentrations (24ppm). However, both HPMC 40-60 and HPMC 10K contribute to the froth formation positively when mixed with NF240 even in low concentration – resulting in a higher recovery of copper without losing too much of the grade in the process. The mechanism of the froth stabilization in these mixture setups is yet unknown. In addition, mixtures of NF240 and HPMC 10K seem to produce better results than mixtures of NF240 and HPMC 40-60. All in all, due to the extremely high flotation kinetics, and the promising behavior of the mixtures, HPMC remains as an interesting chemical in the field of minerals processing, and further efforts to tame its unselective nature are greatly encouraged.

7   Summary & Suggestions for Further Research

In this master's thesis, hydroxypropyl methylcellulose (HPMC) was studied for its potential usage as a flotation frother in chalcopyrite separation from a pyrite rich Cu-Zn ore, and compared to a commercial frother chemical (NF240). In the experimental

section, a total of 53 experiments were conducted utilizing two different types of HPMCs (HPMC 40-60 and HPMC 10K) and NF240, in both a single-frother setup and a mixed-frother setup. Furthermore, the effect of the chemical environment (i.e. the collector and depressant concentrations) to the performance of the frothers were studied as well.

In the experimental part, it was found that:

1) The kinetics of HPMC-based separation are far superior compared to the commercial frother, and very high recoveries were reported

2) HPMC produces very stable but seemingly unselective froths at concentrations exceeding a certain threshold point (around 30ppm)

3) Below the threshold point, HPMC (on its own) produced no or very little froth

4) In the single-frother experiments, HPMC 40-60 and HPMC 10K could not provide separation efficiencies comparable with NF240, due to low copper grades

5) HPMC-based copper separation seems to be somewhat vulnerable to excess frother concentrations, and extremely vulnerable to excess collector concentrations and the choice of pH regulator

6) Mixing HPMC with NF240 was found to have a positive effect on the recovery, without the drastic drop in grade associated with the single-frother HPMC experiments (even at HPMC concentrations well-below the threshold point)

7) Pyrite depression is the main challenge regarding the copper separation from the studied ore

8) In single-frother HPMC experiments, zinc (sphalerite) was often separated even better than copper, despite our efforts of depressing it

Based on these findings, the following suggestions for further research are made:

1) Studying the mixtures of especially HPMC 10K and NF240, in the presence of industrially applied pyrite depressants (cyanide-based)

2) Studying HPMCs with different MS, DS, and DP values in otherwise similar experimental flotation setups, to learn about the effects of these variables to the froth stabilization and selectivity of the chemical

3) Studying the HPMC-based separation of zinc since, in the experiments conducted under this thesis, sphalerite seemed to be concentrated even in the presence of a depressant

4) Studying HPMC-based separation with model ores, to learn about the selectivity of the chemical in a more controlled manner

References

1. Ata, Seher. "Phenomena in the froth phase of flotation—A review." *International Journal of Mineral Processing* 102 (2012): 1-12.

2. Matis, Kostas A., ed. *Flotation science and engineering*. CRC Press, 1994.

3. Reyes-Bozo, Lorenzo, et al. "Assessment of the floatability of chalcopyrite, molybdenite and pyrite using biosolids and their main components as collectors for greening the froth flotation of copper sulphide ores." *Minerals Engineering* 64 (2014): 38-43.

4. Bulatovic, Srdjan M. Handbook of flotation reagents: chemistry, theory and practice: Volume 1: flotation of sulfide ores. Elsevier, 2007.

5. https://pubchem.ncbi.nlm.nih.gov/compound/23683691#section=GHS-Classification. Cited: 07.06.2018.

6. Klemm, Dieter, et al. "Cellulose: fascinating biopolymer and sustainable raw material." *Angewandte Chemie International Edition* 44.22 (2005): 3358-3393.

7. Kamide, Kenji. Cellulose and Cellulose Derivatives. Elsevier Science, 2005.

8. Bock, L. H. "Water-soluble cellulose ethers." *Industrial & Engineering Chemistry* 29.9 (1937): 985-987.

9. Nuorivaara, T., Serna-Guerrero, R. On the remarkable behavior of cellulose surfactant mixtures as froth flotation additives for the recovery of copper from sulfidic tailings. Submitted Manuscript (2018).

10. Wills, Barry A., and James Finch. Wills' mineral processing technology: an introduction to the practical aspects of ore treatment and mineral recovery. Butterworth-Heinemann, 2015.

11. Jávor, Z. 2014. Frother controlled interfacial phenomena in dynamic systems – a holistic approach. Ph.D. Thesis, Aalto University, Espoo, Finland.

12. Fuerstenau, Maurice C., Graeme J. Jameson, and Roe-Hoan Yoon, eds. Froth flotation: a century of innovation. SME, 2007.

13. Bradshaw, Dee. "The role of process mineralogy in improving the process performance of complex sulphide ores." *Proceedings of the XXVII International Mineral Processing Congress*. 2014.

14. Finch, J. A., and C. O. Gomez. "Separability curves from image analysis data." *Minerals Engineering* 2.4 (1989): 565-568.

15. P. S. B. Stewart. "Floatation plant optimisation: metallurgical guide to identifying and solving problems in flotation plants." *Mineral Processing and Extractive Metallurgy*, 119:4 (2010): 247-247, DOI: 10.1179/037195510X12843862943504.

16. Nuorivaara, T. 2015. Rikastushiekan ympäristöominaisuuksien parantaminen vaahdottamalla. M.Sc. Thesis, Aalto University, Espoo, Finland.

17. Schrader, Malcolm E. "Young-dupre revisited." *Langmuir* 11.9 (1995): 3585-3589.

18. Chen, Jian-Hua, Yu-Qiong Li, and Qiu-Rong Long. "Molecular structures and activity of organic depressants for marmatite, jamesonite and pyrite flotation." *Transactions of Nonferrous Metals Society of China* 2010 (2010): 1993-1999.

19. Morris, Gayle E. *The adsorption characteristics of polymeric depressants at the talc-water interface*. Diss. University of South Australia, 1996.

20. Tao, D. "Role of bubble size in flotation of coarse and fine particles—a review." *Separation Science and Technology* 39.4 (2005): 741-760.

21. Zhang, W. 2009. Water overflow rate and bubble surface area flux in flotation. M.Sc. Thesis, McGill University, Montreal, Canada.

22. Jávor, Z., N. Schreithofer, and K. Heiskanen. "Multi-scale analysis of the effect of surfactants on bubble properties." *Minerals Engineering* 99 (2016): 170-178.

23. Cytec Industries Inc. Mining chemicals handbook. *American Cyanamid Company*, New York, 2010.

24. Dai, Zongfu, Daniel Fornasiero, and John Ralston. "Particle–bubble attachment in mineral flotation." *Journal of colloid and interface science* 217.1 (1999): 70-76.

25. Grau, Rodrigo A. *An investigation of the effect of physical and chemical variables on bubble generation and coalescence in laboratory scale flotation cells*. Helsinki University of Technology, 2006.

26. Finch, James A., Jan E. Nesset, and Claudio Acuña. "Role of frother on bubble production and behaviour in flotation." *Minerals Engineering* 21.12-14 (2008): 949-957.

27. Harris, C. C. "Flotation machines." *Flotation--A. M. Gaudin Memorial* (1976).

28. Ahmed, N., and G. J. Jameson. "The effect of bubble size on the rate of flotation of fine particles." *International Journal of Mineral Processing* 14.3 (1985): 195-215.

29. Dobby, G. S., and J. A. Finch. "Particle collection in columns—gas rate and bubble size effects." *Canadian Metallurgical Quarterly* 25.1 (1986): 9-13.

30. Gupta, V. K., et al. "Cellulose: a review as natural, modified and activated carbon adsorbent." *Bioresource technology* 216 (2016): 1066-1076.

31. Wertz, Jean-Luc, Jean P. Mercier, and Olivier Bédué. Cellulose science and technology. EPFL press, 2010.

32. Hallac, Bassem B., and Arthur J. Ragauskas. "Analyzing cellulose degree of polymerization and its relevancy to cellulosic ethanol." *Biofuels, Bioproducts and Biorefining* 5.2 (2011): 215-225.

33. Nishiyama, Yoshiharu, Paul Langan, and Henri Chanzy. "Crystal structure and hydrogen-bonding system in cellulose Iβ from synchrotron X-ray and neutron fiber diffraction." *Journal of the American Chemical Society* 124.31 (2002): 9074-9082.

34. The Cambridge Crystallographic Data Centre (CCDC). Cellulose Iβ: Sample code JINROO01. Access: https://www.ccdc.cam.ac.uk/structures/Search?Ccdcid=JINROO01. Cited: 03.07.2018. Pictures by Tommi Rinne.

35. PubChem: Cellulose. https://pubchem.ncbi.nlm.nih.gov/compound/16211032#section=Solubility. Cited: 28.08.2018.

36. Sahin, Halil Turgut, and Mustafa Burak Arslan. "A study on physical and chemical properties of cellulose paper immersed in various solvent mixtures." *International journal of molecular sciences* 9.1 (2008): 78-88.

37. Akay, Mustafa. *Introduction to Polymer Science and Technology*. Bookboon, 2012.

38. Feller, Robert L., and Myron H. Wilt. *Evaluation of cellulose ethers for conservation*. Getty Publications, 1991.

39. Arisz, Peter W., Hendrikus JJ Kauw, and Jaap J. Boon. "Substituent distribution along the cellulose backbone in O-methylcelluloses using GC and FAB-MS for monomer and oligomer analysis." *Carbohydrate Research* 271.1 (1995): 1-14.

40. Coffey, Donald G., David A. Bell, and Alan Henderson. "Cellulose and cellulose derivatives". *Food polysaccharides and their applications* (2006): 147-180.

41. Ho, Floyd FL, Robert R. Kohler, and George A. Ward. "Determination of molar substitution and degree of substitution of hydroxypropyl cellulose by nuclear magnetic resonance spectrometry." *Analytical Chemistry* 44.1 (1972): 178-181.

42. Vlaia, Lavinia, et al. "Cellulose-Derivatives-Based Hydrogels as Vehicles for Dermal and Transdermal Drug Delivery." *Emerging Concepts in Analysis and Applications of Hydrogels*. InTech, 2016.

43. Salamone, Joseph C., ed. *Concise polymeric materials encyclopedia*. Vol. 1. CRC press, 1998.

44. Wüstenberg, Tanja. *Cellulose and cellulose derivatives in the food industry: fundamentals and applications*. John Wiley & Sons, 2014.

45. Mark, Herman F. *Encyclopedia of polymer science and technology, concise*. John Wiley & Sons, 2013.

46. Urbanski, Tadeusz, Marian/translated by Jurecki, and Sylvia/translated by Laverton. *Chemistry and technology of explosives*. Vol. 2. No. 6. New York, NY: Pergamon Press, 1964.

47. Sigma-Aldrich, Cellulose Nitrate. Available at: https://www.sigmaaldrich.com/catalog/product/aldrich/547964?lang=fi&region=FI&cm_sp=Insite-_-prodRecCold_xviews-_-prodRecCold5-1. Cited: 05.09.2018.

48. Edgar, Kevin J., et al. "Advances in cellulose ester performance and application." *Progress in Polymer Science* 26.9 (2001): 1605-1688.

49. Gedon, Steven, and Richard Fengi. "Cellulose esters, organic esters." *Kirk-Othmer Encyclopedia of Chemical Technology* (2000).

50. Larock, Richard C. *Comprehensive organic transformations: a guide to functional group preparations*. New York: Wiley-vch, 1999.

51. Cheng, H. N., et al. "Synthesis of cellulose acetate from cotton byproducts." *Carbohydrate polymers* 80.2 (2010): 449-452.

52. Yan, Lifeng, et al. "Solvent-free synthesis of cellulose acetate by solid superacid catalysis." *Journal of Polymer Research* 13.5 (2006): 375-378.

53. Heinze, Thomas, Katrin Schwikal, and Susann Barthel. "Ionic liquids as reaction medium in cellulose functionalization." *Macromolecular bioscience* 5.6 (2005): 520-525.

54. Das, Archana M., Abdul A. Ali, and Manash P. Hazarika. "Synthesis and characterization of cellulose acetate from rice husk: Eco-friendly condition." *Carbohydrate polymers* 112 (2014): 342-349.

55. Sigma-Aldrich, Cellulose Acetate. Available at: https://www.sigmaaldrich.com/catalog/substance/celluloseacetate123459004 35711?lang=fi&region=FI. Cited: 03.09.2018.

56. Vatankhah, Elham, et al. "Development of nanofibrous cellulose acetate/gelatin skin substitutes for variety wound treatment applications." *Journal of biomaterials applications* 28.6 (2014): 909-921.

57. Adelstein, Peter Z., et al. "Stability of cellulose ester base photographic film: Part I—Laboratory testing procedures." *SMPTE journal* 101.5 (1992): 336-346.

58. Thielking, Heiko, and Marc Schmidt. "Cellulose ethers." *Ullmann's encyclopedia of industrial chemistry* (2006).

59. Klemm, Dieter, et al. *Comprehensive cellulose chemistry. Volume 2: Functionalization of cellulose*. Wiley-VCH Verlag GmbH, 2004.

60. Feller, Robert L., and Myron H. Wilt. *Evaluation of cellulose ethers for conservation*. Getty Publications, 1991.

61. Chemical Economics Handbook: Cellulose Ethers. IHS Markit. 2016. Available at: https://ihsmarkit.com/products/cellulose-ethers-chemical-economics-handbook.html. Cited: 30.08.2018.h

62. Arboleya, Juan-Carlos, and Peter J. Wilde. "Competitive adsorption of proteins with methylcellulose and hydroxypropyl methylcellulose." *Food Hydrocolloids* 19.3 (2005): 485-491.

63. Heinze, Thomas, Omar A. El Seoud, and Andreas Koschella. *Cellulose derivatives: synthesis, structure, and properties*. Springer, 2018.

64. Phadtare, Dipti, et al. "Hypromellose—a choice of polymer in extended release tablet formulation." *World J Pharm Pharm Sci* 3 (2014): 551-566.

65. Sigma-Aldrich, Hypromellose. Available at: https://www.sigmaaldrich.com/catalog/substance/hypromellose12345900465311?lang=fi&region=FI. Cited: 27.06.2018.

66. Sahoo, Chinmaya Keshari, Surepalli Ram Mohan Rao, and M. Sudhaka. "HPMC a biomedical polymer in pharmaceutical dosage forms." *J Chem Pharm Sci* 8 (2015): 875-81.

67. Karlsson, Kristina, et al. "Foaming behavior of water-soluble cellulose derivatives: hydroxypropyl methylcellulose and ethyl hydroxyethyl cellulose." *Cellulose* 22.4 (2015): 2651-2664.

68. De Moura, M. R., et al. "Properties of novel hydroxypropyl methylcellulose films containing chitosan nanoparticles." *Journal of food science* 73.7 (2008): N31-N37.

69. Camino, Nerina A., et al. "Hydroxypropylmethylcellulose surface activity at equilibrium and adsorption dynamics at the air–water and oil–water interfaces." *Food Hydrocolloids* 23.8 (2009): 2359-2368.

70. Ghanbari, M., and J. Farmani. "Influence of hydrocolloids on dough properties and quality of barbari: an Iranian leavened flat bread." *Journal of Agricultural Science and Technology* 15.3 (2013): 545-555.

71. Gurumoorthy, Anand VP, and K. H. Khan. "Polymers at interfaces: biological and non-biological applications." *Recent Research in Science and Technology* 3.2 (2011).

72. Nahringbauer, Inger. "Dynamic surface tension of aqueous polymer solutions, I: ethyl (hydroxyethyl) cellulose (BERMOCOLL cst-103)." *Journal of Colloid and Interface Science* 176.2 (1995): 318-328.

73. Shen, Wei Zhong, Daniel Fornasiero, and John Ralston. "Flotation of sphalerite and pyrite in the presence of sodium sulfite." *International Journal of Mineral Processing* 63.1 (2001): 17-28.

74. Stauter, John C. "Pyrite depression in coal flotation by the addition of sodium sulfite." U.S. Patent No. 3,919,080. 11 Nov. 1975.

75. Mu, Yufan, Yongjun Peng, and Rolf A. Lauten. "The depression of pyrite in selective flotation by different reagent systems–A Literature review." *Minerals Engineering* 96 (2016): 143-156.

76. Boulton, Adrian, Daniel Fornasiero, and John Ralston. "Selective depression of pyrite with polyacrylamide polymers." *International Journal of Mineral Processing* 61.1 (2001): 13-22.

77. Önal, G., et al. "Flotation of Aladag oxide lead–zinc ores." *Minerals Engineering* 18.2 (2005): 279-282.

Milling Ball Diameter [mm]	Number of Balls
39	3
28	18
23	24
16	27

In this appendix, all masses of added water are marked for each flotation experiment (excluding the Quartz flotation tests, which can be found from chapter 5.3). During the experiments, the water additions were always performed immediately after the fractions were completed, excluding the ones in which short time intervals were used. Therefore, for example in "PRA Flota 1", the water addition of 39.2g has been done at time t=3min. For the short time interval experiments, the first water addition was also done at time t=3min, after the first 5 fractions had been collected. The experiments, in which short intervals were utilized, are marked with red on this appendix. All water masses are marked in grams.

	0-3min / 0-30s [g]	3-6min / 30-60s [g]	6-10min / 60-90s [g]	10-14min / 90-120s [g]	14-20min / 120-150s [g]	20-30min / 3-6min [g]	Total [g]
PRA Flota 1	39.2	65.1	48	30.5	0	0	182.8
PRA Flota 4	159.3	167.3	149.7	125.8	142.8	153.3	898.2
PRA Flota 13	32.5	98.2	37.6	25.8	85.6	36.3	316
PRA Flota 16	213.7	169.7	154.3	79.7	95.6	98.4	811.4
PRA Flota 22	0	0	0	0	0	0	0
PRA Flota 23	57.8	0	0	0	0	0	57.8
PRA Flota 26	187.4	57.4	34.8	70.2	120.7	197.2	667.7
PRA Flota 28	259.6	184.6	116	119.3	110.7	0	790.2
Pre-Thesis Flota 1	42.8	87.5	94.8	82.1	210.7	159	676.9
Pre-Thesis Flota 2	53.4	55.3	56.4	117.6	161.3	192.1	636.1
Pre-Thesis Flota 3	97	70.6	73.5	77.4	121	190.2	629.7

Pre-Thesis Flota 4	50	41.1	20.2	97.8	139.4	161	509.5
Pre-Thesis Flota 5	42.8	44.4	93.5	118.7	136.8	137.6	573.8
Pre-Thesis Flota 6	145.7	120.3	96.5	132.5	127.7	127.3	750
Pre-Thesis Flota 7	200.6	93.7	155	115.4	128.9	100.3	793.9
Pre-Thesis Flota 8	0	0	0	0	0	0	0
Pre-Thesis Flota 9	0	0	0	0	0	0	0
Pre-Thesis Flota 10	0	0	0	0	0	0	0
Pre-Thesis Flota 11	515.6	0	0	0	0	0	515.6
Pre-Thesis Flota 12	368	172.1	0	0	0	0	540.1
Pre-Thesis Flota 13	573.2	0	0	0	0	0	573.2
Pre-Thesis Flota 14	660.5	0	0	0	0	0	660.5
Pre-Thesis Flota 15	401.7	0	0	0	0	0	401.7
Thesis Flota 1	0	0	0	0	73.8	0	73.8
Thesis Flota 2	0	0	0	0	433.1	0	433.1
Thesis Flota 3	0	0	0	0	354.5	0	354.5
Thesis Flota 4	0	0	0	0	331.5	0	331.5
Thesis Flota 5	0	0	0	0	0	0	0
Thesis Flota 6	0	0	0	0	180	0	180
Thesis Flota 7	0	0	0	0	619.5		619.5
Thesis Flota 8	167	115.1	117.5	156.4	104.6	125.4	786
Thesis Flota 9	152	177.7	184.8	66.9	100.5	105.6	787.5
Thesis Flota 10	0	0	0	0	0	0	0
Thesis Flota 11	0	0	0	0	164.2	0	164.2
Thesis Flota 12	0	0	0	0	269.1	48	317.1
Thesis Flota 13	0	0	0	0	250	0	250
Thesis Flota 14	176.2	247.3	45.4	126.4	118.6	0	713.9
Thesis Flota 15	128.8	20.2	255	151.4	127.1	0	682.5
Thesis Flota 16	165.4	148.4	162.5	210.5	111.5	0	798.3

Thesis Flota 17	124.7	112.7	287.2	131.6	130.9	69.3	856.4
Thesis Flota 18	0	0	0	0	172.4	186.2	358.6
Thesis Flota 19	0	0	0	0	222.4	141.3	363.7
Thesis Flota 20	90	98.1	100.9	169.3	189.4	121.9	769.6
Thesis Flota 30	106.5	0	0	0	0	0	106.5
Thesis Flota 31	94.8	88.7	130.9	196.3	159.3	130.7	800.7
Thesis Flota 32	152.2	119.1	147.3	190.3	115.1	184.3	908.3
Thesis Flota 33	225.9	174.2	210	82.6	106.1	382.4	1181.2
Thesis Flota 34	253.2	304.5	239.6	0	0	0	797.3
Thesis Flota 35	160	168.9	192	110.1	127.2	131.7	889.9
Thesis Flota 36	108.2	181.2	209.5	98.1	134.1	173.9	905
Thesis Flota 37	127	184.9	206.7	107.2	173.1	172.9	971.8

This appendix shows the fraction-specific copper grades in each "Thesis Flotation" experiment. The experiments, in which short intervals were utilized, are marked with red on this appendix. All copper grades are marked in percentages.

	0-3min / 0-30s	3-6min / 30-60s	6-10min / 60-90s	10-14min / 90-120s	14-20min / 120-150s	20-30min / 3-6min	Tailings
Thesis Flota 1	0,34 %	0,42 %	0,41 %	0,45 %	0,42 %	0,47 %	1,12 %
Thesis Flota 2	2,76 %	2,53 %	2,36 %	2,36 %	2,34 %	2,27 %	0,47 %
Thesis Flota 3	4,50 %	4,06 %	3,58 %	3,36 %	3,18 %	2,53 %	0,39 %
Thesis Flota 4	2,39 %	2,19 %	2,11 %	1,88 %	1,95 %	1,81 %	0,54 %
Thesis Flota 5	3,66 %	3,94 %	3,69 %	3,51 %	3,43 %	0,00 %	0,82 %
Thesis Flota 6	2,77 %	2,73 %	2,70 %	2,71 %	2,65 %	2,39 %	0,94 %
Thesis Flota 7	2,24 %	2,23 %	2,08 %	2,05 %	2,23 %	1,84 %	0,82 %
Thesis Flota 8	0,48 %	2,84 %	2,71 %	2,11 %	1,90 %	1,24 %	0,90 %
Thesis Flota 9	0,00 %	0,00 %	0,00 %	0,00 %	0,00 %	0,00 %	0,00 %
Thesis Flota 10	1,64 %	1,41 %	1,12 %				0,65 %
Thesis Flota 11	1,64 %	1,23 %	1,22 %	1,35 %	1,72 %	2,06 %	0,42 %
Thesis Flota 12	1,14 %	0,80 %	0,79 %	0,97 %	1,12 %	1,38 %	0,16 %
Thesis Flota 13	3,06 %	1,94 %	1,26 %	1,09 %	0,95 %	1,25 %	0,24 %
Thesis Flota 14	0,93 %	2,32 %	6,80 %	8,32 %	6,93 %	3,28 %	0,34 %
Thesis Flota 15	1,12 %	2,69 %	7,52 %	6,13 %	4,55 %	1,90 %	0,29 %
Thesis Flota 16	1,67 %	7,38 %	7,93 %	3,91 %	2,95 %	1,38 %	0,17 %
Thesis Flota 17	1,27 %	7,21 %	9,07 %	4,48 %	3,08 %	0,87 %	0,23 %
Thesis Flota 18	0,84 %	0,19 %	0,10 %	0,08 %	0,10 %	0,40 %	1,03 %

Thesis Flota 19	0,10 %	0,07 %	0,07 %	0,10 %	0,18 %	0,77 %	0,99 %
Thesis Flota 20	1,43 %	5,48 %	7,06 %	4,13 %	2,67 %	1,49 %	0,17 %
Thesis Flota 30	0,29 %	0,00 %	0,00 %	0,00 %	0,00 %	0,00 %	0,782 %
Thesis Flota 31	1,34 %	8,58 %	7,58 %	3,97 %	2,37 %	1,42 %	0,271 %
Thesis Flota 32	1,27 %	5,19 %	4,85 %	2,92 %	1,56 %	0,65 %	0,062 %
Thesis Flota 33	0,92 %	4,31 %	3,97 %	2,10 %	1,00 %	0,55 %	0,073 %
Thesis Flota 34	0,60 %	0,92 %	1,37 %	0,00 %	0,00 %	0,00 %	0,834 %
Thesis Flota 35	1,52 %	5,76 %	5,59 %	3,80 %	1,95 %	1,13 %	0,101 %
Thesis Flota 36	1,42 %	5,56 %	6,80 %	4,71 %	2,62 %	1,48 %	0,119 %
Thesis Flota 37	1,78 %	6,83 %	5,55 %	3,76 %	2,00 %	1,42 %	0,152 %